EFFECT OF CHITOSAN LACTATE ON THE FORMATION OF CHITOSAN-DNA PARTICLES

A PHYSICOCHEMICAL, HAEMOCOMPATIBLE AND CYTOTOXIC STUDY

Hélder Tão Ferraz Cardoso Soares

Dissertação apresentada para provas de Mestrado em Química, área de especialização em Processos Químicos Industriais

Professora Dr. Maria da Graça Miguel

Doutora Maria del Carmen Morán

Setembro de 2011

Universidade de Coimbra

Acknowledgments

This thesis could not be done without the help of all the people involved in this work. Sometimes the path could be tough and I considered myself fortunate, for be surrounded with the right persons that show me the correct way to follow. So, I would like to express a few words of gratitude to

Professora Maria G. Miguel por me ter dado a oportunidade de trabalhar no seu grupo de investigação. Por todo o apoio prestado e pelo conhecimento científico transmitido.

Doutora Carmen Morán pela amizade, pelo ambiente descontraído e de constante aprendizagem que sempre foste capaz de transmitir. Por mesmo estando longe nunca teres deixado de estar presente. Muito desta tese se deve ao teu incentivo.

Professor Björn Lindman for all the fruitful discussions and the availability to share your ideas about the work.

Grupo de Colóides ao Filipe, pela amizade, pelo interesse, ajuda e disponibilidade que sempre demonstraste, foi um prazer trabalhar contigo, ao Fafe pelo companheirismo e apoio prestado, ao Bruno, ao Tiago, à Salomé, obrigado pela tua ajuda e importante contributo na realização desta tese, à Marta, à Rita, à Cláudia e à Tânia. À Andreia que não fazendo parte do grupo de Colóides foi uma ajuda muito importante.

Pessoal da Casa Olá ao Nélson, à Di, ao Renato e ao Gonçalo, obrigado pela vossa ajuda e interesse no trabalho, ao Noddy, ao Camon, ao João e ao Rui.

Amigos de Coimbra ao César, à Rita, à Angela e à Marta, sem a vossa amizade este percurso não tinha significado.

Amigos de Ermesinde ao Samuel, ao Pedro, à Vera, ao Satan, ao Bino e ao Xano pelos bons momentos que passamos sempre que estamos juntos.

Família às minhas irmãs Catarina e Cláudia, pelo apoio, pela amizade que nos une, pelo exemplo que são para mim, à Mónica pelos momentos que vivemos juntos, pela força que só tu me consegues dar. Por seres o meu porto de abrigo, sem ti nada fazia sentido. Aos meus Pais, pelo carinho e amor incondicional, por terem compreendido a minha decisão de vir para Coimbra. Sei bem o que isso custou e por isso esta tese também é vossa.

Table of contents

Abbreviations

(By order of appearance)

DNA – Deoxyribonucleic acid

G.C. – Guanine Cytosine

T_m – melting temperature

Bp – Base par

NMR – Nuclear Magnetic Resonance

LD_{50} – Lethal Dosis 50%

Mw – Molecular weight

DD – Degree of deacetylation

nm – Nanometers

mM – miliMolar

CL – Chitosan Oligossacharide Lactate

dsDNA – Double stranded DNA

ssDNA – Single stranded DNA

CTAB – Cetyl trimethylammonium bromide

FM – Fluorescence Microscopy

SEM – Scanning Electron Microscopy

AO – Acridine Orange

LC – Loading Capacity

UV -Vis – Ultra Violet-Visible

PCS – Photon Correlation Microscopy

MWCO – Molecular weight cut off

NP - Nanoparticles

SE – Standard Error

LC_{50} – Lethal Concentration 50%

S_1 – Singlet excited state

S_0 – Ground state

FRET – Fluorescence Resonance Energy Transfer

BSE – Backscattered Electron

EBSD – Diffracted Backscattered Electron

HOMO – Highest Occupied Molecular Orbital

LUMO – Lowest Unoccupied Molecular Orbital

DLS – Dynamic Light Scattering

QLS – Quasielastic Light Scattering

λ – Wavelenght

I0 – Incident Intensity

TBE – TrisBorate-EDTA

LDH – Lactate dehydrogenase

NR – Neutral Red

DMSO – Dimethyl Sulfoxide

PBS – Phosphate buffered saline

Resumo

Este relatório pretende demonstrar o trabalho desenvolvido ao longo do último ano e meio, no que respeita à temática de Encapsulação de DNA, usando para o efeito Partículas de Gel e Nanopartículas.

O trabalho a que se refere este relatório incidiu na criação de partículas de gel, preparadas por gelificação na interface água/água, através da interacção de dois polielectrólitos de carga oposta, o DNA e um oligossacarídeo de baixo peso molecular, o lactato de quitosano. É de destacar que as partículas foram obtidas sem utilizar agentes quelantes (cross-linkers), ou solventes orgânicos. Numa segunda parte do trabalho procedeu-se à experimentação de nanopartículas de Lactato de Quitosano contendo DNA no seu interior, usando para o efeito um nebulizador, que permitiu originar pequenas gotículas de DNA.

De modo a caracterizar os sistemas obtidos, estes foram estudados através de uma análise de vários parâmetros físico-químicos: morfologia e estrutura das partículas assim como o grau de complexação sofrida pela gota de DNA, cinéticas de libertação de DNA por forma a comprovar a sua estabilidade, viscosidade dos polielectrólitos de forma a poder obter partículas de gel estáveis, tamanho e a carga das partículas, estudo o qual derivou na abordagem às Nanopartículas, uma vez que estas permitiriam uma transfecção celular mais eficaz. Foi também estudado, na Facultat de Farmacia em Barcelona, o efeito de tanto o Lactato de Quitosano como as partículas obtidas, na viabilidade celular através de ensaios com sal *tetrazolium MTT* em linhas celulares do tipo *3T3 fibroblast*, bem como a interacção destes, com outros modelos celulares mais simples como os eritrócitos.

Estes estudos permitiram verificar que o Lactato de Quitosano é um promissor agente no que respeita à transferência de genes.

Abstract

This report aims to demonstrate the study conducted over the last year and a half, concerning the DNA encapsulation theme, by using gel particles and nanoparticles.

The study this report refers focused on the creation of gel particles, prepared by gelification in the water/water interface, through the interaction between two polyelectrolytes of opposing charges, the DNA and an oligosaccharide of low molecular weight, the Chitosan Lactate. It should be pointed out that the particles were obtained without the use of cross-linkers or organic solvents. In a second portion of the study, the experimentation of the Chitosan Lactate nanoparticles containing DNA inside was conducted using a nebulizer which allowed small DNA droplets to form.

In order to characterize the obtained systems, they were studied through an analysis of several physicochemical parameters: particle morphology and structure as well as the degree of complexation endured by the DNA drop, DNA release kinetics, so as to ensure its stability, polyelectrolyte viscosity in order to obtain stable gel particles, particle size and charge which lead to the study of nanoparticles, since these allowed for a more effective cell transfection. The effect of the Chitosan Lactate, as well as the obtained particles, on cell feasibility was also studied, on the Facultat de Farmacia in Barcelona, with tetrazolium salt MTT assay in 3T3 fibroblast cell lines and also the interaction between Chitosan Lactate and simpler cell models such as erythrocytes.

These studies allowed the verification of the Chitosan Lactate as a promising gene carrier.

Chapter 1.

Introduction

1.1 Polyelectrolytes

Polyelectrolytes, schematically represented in Figure 1, are macromolecules that have ionic groups along their chains, that is, polyelectrolytes are not more than polymers that contain monomer units with electric charge.

Polyelectrolytes have a dual nature, since they are both polymers, with respect to the molecular chain, and electrolytes due to high charge density. Polyelectrolytes have unique characteristics that come from the electrostatic interactions between ionized groups and non-ionized, counter-ions and solvent molecules, that are naturally, very sensitive to both the structure of the polymer and the chemical environment that surrounds it (*1*).

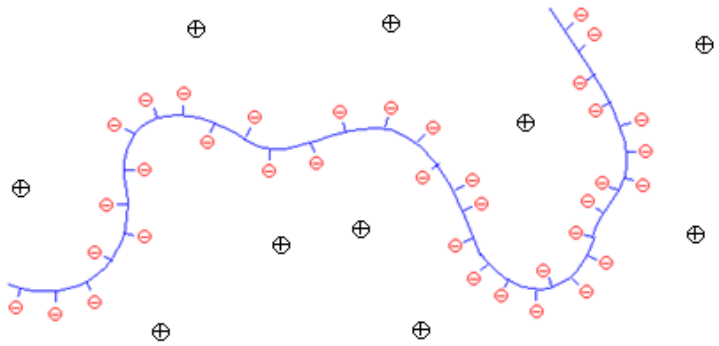

Figure 1 - Illustrative image of an anionic polyelectrolyte expanded due to repulsion of charges.

The ionic groups of the polyelectrolyte can dissociate completely when dissolved in water (polybasic / strong polyacid) or partially (polybasic / weak polyacid), which can be described in terms of *pKa* or *pKb* (*2*).

Regarding the charge, polyelectrolytes can be divided in three groups:
- Cationic, positively charged;

- Anionic, negatively charged;

- Non-ionic, that are not polyelectrolytes in the strict sense, but, in solution, have similar characteristics to the polyelectrolytes.

Electrostatic interactions between charges lead to the rich behavior of polyelectrolyte solutions, qualitatively different from those of uncharged polymers(*3-4*) , for example:

(1) The crossover from dilute to semidilute solution regime occurs at much lower polymer concentrations than that in solutions of neutral chains.

(2) There is a well-pronounced peak in the scattering function of the homogeneous polyelectrolyte solutions. The magnitude of the wave vector corresponding to this peak increases with concentration as $c^{1/2}$. There is no such peak in solutions of neutral polymers.

(3) Polyelectrolyte chains in semidilute regime follow unentangled dynamics in a much wider concentration range and the crossover to the entangled dynamics occurs further away, from the chain overlap concentration than in solutions of uncharged polymers.

Numerous molecules with high biological importance and many synthetic polymers are polyelectrolytes. Since the polypeptides to the polyacrylic acid (PAA), there are many examples of polyelectrolytes, but none have such a central role in life as DNA.

1.2 DNA as a biological polyelectrolyte

Deoxyribonucleic acid (DNA) is an organic compound polymer that contains the genetic instructions used in the development and functioning of all known living organisms and some viruses.

From the chemical point of view, DNA is a long polymer of simple units (monomers) of nucleotides, with two "strands" (backbone) made of sugars and phosphate groups joined by ester bonds. These two strands run in opposite directions to each other, forming a double helix, and are therefore anti-parallel.

Attached to each sugar is one of four nucleobases and is this sequence of bases along the backbone that encodes information. So, the DNA molecule contains four different bases: two purines (adenine and guanine) and two pyrimidines (cytosine and thymine), which are represented in Figure 2.

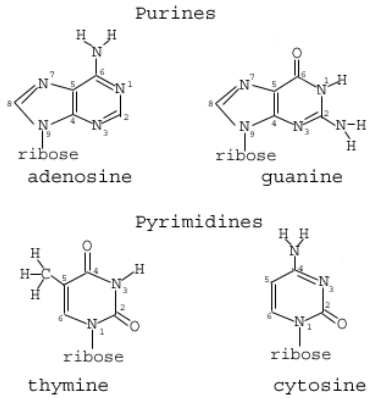

Figure 2 – DNA bases (Adapted from reference (*5*)).

The diameter of the helix is approximately 20 Å. According to the Watson and Crick model, the polynucleotide strands are wound like a double helix around an imaginary axis, where the two strands are held together by hydrogen-bonding bridges between internally located bases(*6*). Each adenine must be paired with a

thymine and each guanine with a cytosine, separated by 3.4 Å along the chain and related by a rotation of 36 degrees. The sequence of the bases along the polynucleotide chain is not restricted in any way, and the precise sequence of bases carries the genetic information(*6*). Nowadays, it is realized that the structure of the double helical DNA can vary as seen in Figure 3.

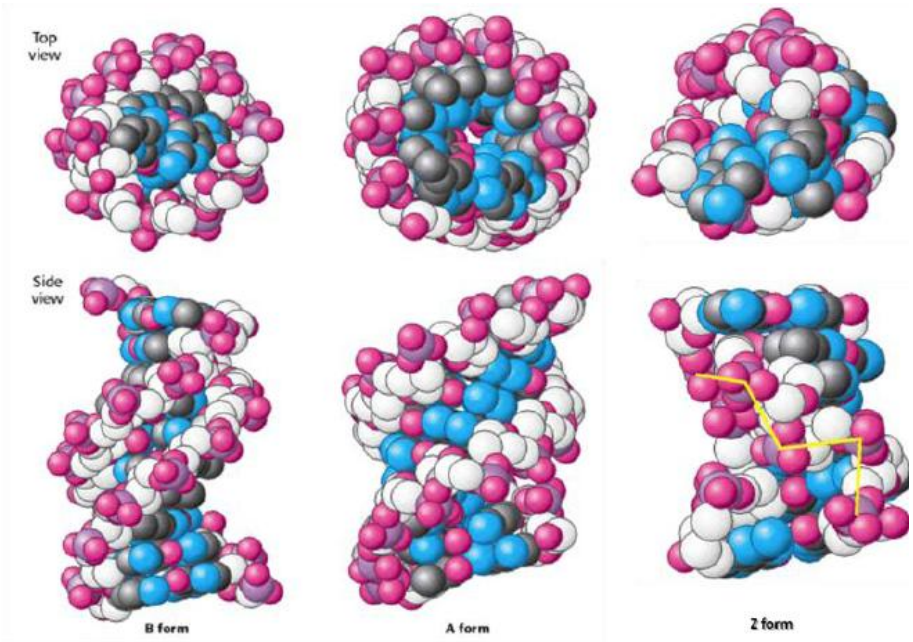

Figure 3 - Secondary structures corresponding to the different A, B and Z DNA conformations (adapted from reference(*7*)). The carbon atoms of the backbone are shown in white.

Under physiological conditions, at low salt concentration (150 mM), B-DNA is the most stable structure. However, the two other structures, represented in Figure 3, have been well characterized in crystallographic studies and are believed to occur in nature. The general observation is that A-DNA is favored upon dehydration and when the repulsion along the helix is reduced(*8*). A-DNA, like B-DNA, is a right-handed double helix consisting of antiparallel strands held together by base pairs. The A helix is wider and shorter than the B helix, and the

respective base pairs are tilted rather than perpendicular to the helix axes. In the third form the phosphates in the backbone zigzagged, and that is why it is called Z- DNA. The Z-form presents a left-handed helix, in contrast with the right-handed screw sense of the A and B helices. All the nucleotides along B-DNA have the same conformation, whereas in left-handed helix they alternate between *syn* and *anti* conformations of the bases. Since the *syn* conformation is more stable for purines than for pyrimidines, this form is favored in nucleotide sequences that have alternations of purines and pyrimidines. In physiological conditions, the Z-DNA form is less stable than B-DNA because of the higher electrostatic repulsion between closer phosphate groups(*9*). However the biological role of Z-DNA transient conformation is still under investigation.

Based on the structure of the double helix and also on the hydrophobicity characteristics, the structure of DNA is as follows:

-The sugar and the phosphate groups (hydrophilic part) are located on the external part of the molecule;

-The nucleobases (hydrophobic part) are located on the internal part of the molecule.

DNA´s double-helix is kept stable by two types of interactions:

-Hydrogen bonding established by the complementary bases;

-Hydrophobic interactions, that forces the bases to "hide" inside the double-helix.

Knowing that at a physiological pH the ester bonds that connect all the monomers are fully ionized, we can see why the DNA is considered a poly-anion, which usually has an associated alkyl counter-ion. Once a polyelectrolyte is a polyion coupled to the counter-ions surrounding it, DNA is seen as a polyelectrolyte (*10*).

When a solution of DNA is heated above a certain temperature, its native form undergoes a physical process where complementary chains are separated from each other and assume a random coil configuration.

This important process is known as denaturation (Figure 4) and leads to qualitative and quantitative differences in the physical properties of DNA(*11*).

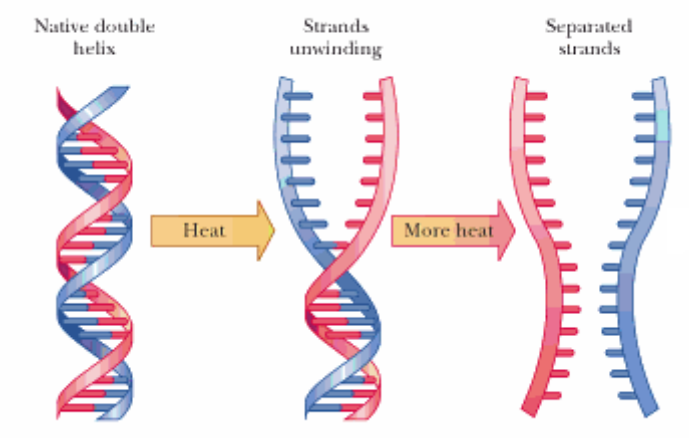

Figure 4 – Schematic DNA denaturation process. (Adapted from reference (*12*)).

The best way of following denaturation is through ultraviolet (UV) absorbance. When DNA denatures, a hyperchromic effect (increase in the absorbance intensity) by approximately 40% is noted in its characteristic UV spectrum. By monitoring this effect, at a specific wavelength (260 nm), as a function of the temperature a sigmoid curve is obtained, giving indication that the denaturation of dsDNA is a cooperative phenomenon. This curve is called melting curve and the temperature at its midpoint is known as DNA melting temperature, T_m (Figure 5). Thus T_m is a measure of DNA double helix stability in solution.DNA double helix stability in solution is dependent on several factors, such as the nature of the solvent, ionic strength, counterion identity, G.C. (guanine cytosine) base par content and pH.

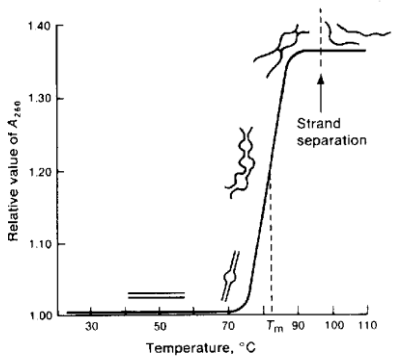

Figure 5 – Example of a DNA melting curve.

1.3 Gene Delivery

Ever since the discovery of the basic structure and function of the human genome, the use of gene products as therapy for both hereditary and acquired diseases has been an important goal for biomedical research. Although the objectives and principles of gene therapy have been well-defined over the last decades, the respective application as a versatile, therapeutically successful approach has not yet met expectations. Depending on the vectors used for nucleic acid transfer, gene delivery is roughly divided into two main categories: viral and non-viral delivery(*13*). Viral vectors, which include retroviruses, adenoviruses, and adeno-associated viruses, are highly specialized organisms, which have developed numerous ways of invading the cells to the body. This makes them highly suitable as efficient gene transfer vectors. However, an increasing concern about immune responses(*14*) to viral vectors *in vivo* combined with the ease of production and versatility of plasmids *in vitro* opens the door for non-viral vector development.

Non-viral vectors usually consist of cationic polymers (polyplexes) or cationic lipids (lypoplexes). The cationic charge of these molecules enables the electrostatic interactions with negatively charged DNA. Although non-viral possess lower immunogenic than their viral counterparts. Other advantages of non-viral vectors include ease of synthesis and the possibility for repeatable administration with minimal host immune response. Large scale production is also easier compared to viral vectors and due to the larger size, more DNA can be packaged to non-viral carriers (*15-16*).

Nevertheless, the transfection efficiency mediated by these non-viral gene delivery vectors has to be improved so that applications may fully benefit from the advantages of the technique. Gene therapy has turned attention to DNA-polycation complexes as promising novel systems for drug delivery, so a physical understanding of the DNA-polycation interaction has became crucial to the rational design of what is being called "artificial viruses" (*17-18*).

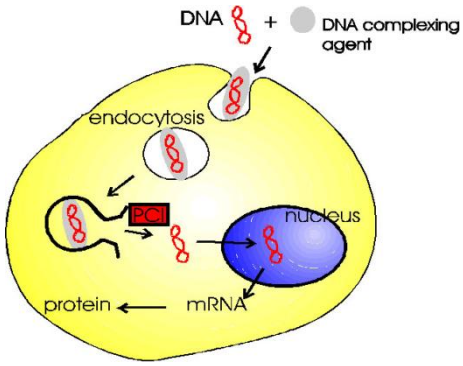

Figure 6 – Mechanism of DNA delivery into the cells. (Adapted from reference(*19*)).

Nowadays, the work on the encapsulation and compaction of DNA into cells and its relationship with the transcription machinery remains a subject of great interest, with a long way to go to a full understanding of this subject.

The compaction of DNA, along with the charge reduction facilitates the delivery of nucleic acids through cell membranes(*2*) (Figure 6). Once a strong bond of cationic entities with DNA induces these effects, it is easy to understand why the use of complexation with lipids, cationic surfactants or polysaccharides, such as chitosan, as a major strategy for the delivery of DNA into cells.

1.4 Chitosan: physicochemical properties

Chitosan is a linear polysaccharide composed of randomly distributed chains of β-(1-4) D-glucosamine (deacetylated unit) and N-acetyl-D-glucosamine (acetylated unit).

It is produced commercially by deacetylation of chitin, which is a structural element of the exoskeleton of crustaceans and is the second most natural abundant polymer immediately after cellulose. The degree of deacetylation can be determined by NMR spectroscopy and the percentage varies between 60-100%.

By hydrolysis, chitosan can give rise to an oligosaccharide of low molecular weight. (Figure 7)

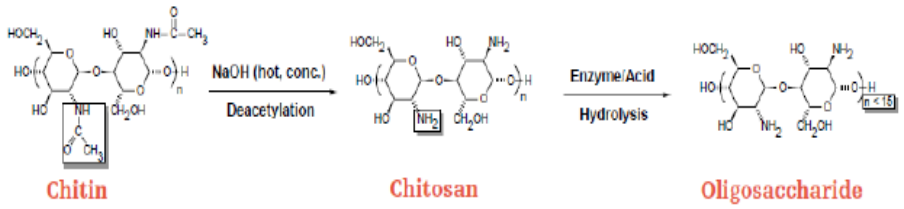

Figure 7 – Structure of chitin and the reactions that lead to the chitosan and to the corresponding oligossacharide. (Adapted from Sigma-Aldrich products section).

Chitosan contains amino groups with a pKa value of 6.2-7 and it is considered as a strong base(*20-21*). Chitosan is soluble in dilute acidic solutions at pH below 6. It can also form water-soluble salts, such as chitosan acetate and chitosan lactate, with some aqueous inorganic or organic salts(*22*). The solubility of chitosan generally increases as pH decreases. This is because at low pH the amino groups of chitosan get protonated resulting in a water soluble cationic polyelectrolyte(*20, 22*). In these conditions the surface charge of chitosan is positive, allowing it to interact with negatively charged surfaces. However, if pH is higher than 6, the amines become deprotonated and lose their charge, resulting in a neutral insoluble polymer. At physiological pH 7.4 chitosan has low solubility in aqueous solutions. To overcome this problem, many soluble chitosan derivatives have been developed by modifying the reactive functional groups of chitosan or by depolymerising the chitosan (*23*).

Chitosan has a wide number of useful properties because it is biocompatible, antibacterial and also an environmentally-friendly polyelectrolyte, which lead to numerous applications in various areas, including processing water, additives for cosmetics, textile treatment components, biomedical equipments and microcapsules for controlled drug delivery (*24-26*).

1.4.1 Chitosan Biocompatibility

Chitosan is generally considered biocompatible both in vitro and in vivo conditions. This property is somewhat attributable to factors such as the natural source, molecular weight, degree of deacetylation (DD), and especially the preparation method.(*27*)

The cytocompatibility of chitosan has been reported in vitro with ephithelial and myocardial cells. In addition, chitosan is cytocompatible with fibroblasts, chondrocytes, hepatocytes and keratinocytes.

Chitosan is also haemocompatible and it has been reported as a coagulating factor, both in vivo and in vitro. In vitro chitosan maintains its coagulating properties even in severe anticoagulating conditions and in the presence of abnormal activity by platelets. In mice the LD_{50} *(*Lethal Dosis 50%) of directly injected chitosan is 10mg/day/Kg body weight. However, high doses (200 mg/Kg) have been reported to lead to hemorrhagic pneumonia in dogs (*28*).

As a whole, chitosan can be regarded as non-toxic when administered in appropriate amounts.

1.4.2 Chitosan as a non-viral vector for gene delivery

Mumper et al were the first to report the use of chitosan as a gene delivery system in 1995(*29*). Since then, numerous authors have reported studies on chitosan as a non-viral vector for DNA. The potential of chitosan as a gene delivery carrier is based on its cationic property. In addition chitosan is relatively cheap and readily available. Most commonly, chitosan has been complexed with DNA by ionic interaction between the negatively charged backbone of DNA and the positively charged amine groups of chitosan. These interactions results in a stable complex, in which the chitosan protects the DNA from nuclease degradation. (Figure 8)

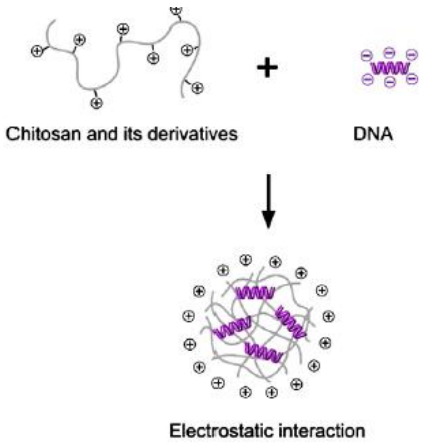

Figure 8 – Illustrative image of the interaction between Chitosan or its derivatives and DNA. (Adapted from reference (*16*)).

Previous studies have shown that the binding affinity of chitosan for DNA, the stability and the transfection efficiency of the chitosan/DNA complexes are dependent on several formulation parameters, such as the molecular weight (Mw) of chitosan, degree of deacetylation (DD), stoichiometry of the chitosan/DNA complex, cell type and so on(*30-32*). The variation in these parameters can influence the size, charge, cell uptake and release of the chitosan/DNA complex, hence the overall transfection efficacy. Therefore, they must be considered carefully when designing a gene therapy system.

1.4.3 Impact of molecular weight and degree of deacetylation

The Mw of chitosan is an important factor that influences particle size, chitosan/DNA complex stability, the efficiency of cell uptake, the dissociation of DNA from the complex after endocytosis, and therefore the transfection efficiency of the complex (*33-34*).

Based on the literature, high Mw chitosans are superior to those with low Mw in enhancing the stability of complexes, which is beneficial for the protection of DNA in the cellular endosomal/lysosomal compartments. On the other hand, high Mw chitosans restrict the release of DNA once inside the cells, resulting in low or delayed expression. In contrast, complexes formed with chitosans of rather low Mw are not sufficiently stable and cannot provide effective protection for DNA due to early dissociation and therefore show little or no transgene expression. Consequently, an intermediate degree of stability needs to be achieved with chitosan molecules of an appropriate Mw between extracellular DNA protection (better with high Mw) versus efficient intracellular DNA release (better with low Mw) in order to obtain high levels of transfection (*35-36*).

The degree of chitosan deacetylation (DD) is the percentage of deacetylated primary amine groups along the molecular chain. Higher DD results in the increase of positive charge, enabling a greater DNA binding capacity and cellular uptake. In addition, the DD of chitosan influences its solubility, crystallinity, and degradation (*37*).

1.5 Interaction between oppositely charged systems

The phase behavior of polymer-surfactant, surfactant-surfactant and polymer-surfactant systems is primarily through the same type of interactions. Depending on the interaction between the two entities, the phase behavior can show segregative phase separation, associative phase separation, or miscibility(*38*).

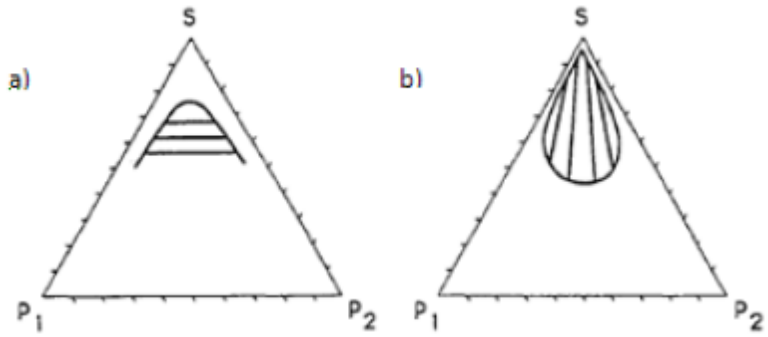

Figure 9 - Ternary diagrams where a) segregative phase separation; b) associative phase separation. P1 and P2 are polymers and S is a solvent common to both. (Adapted from reference(*39*))

When the interaction is repulsive, there is a greater tendency to have a segregative phase separation, on the contrary, when there is an attractive interaction it may result in associative phase separation or miscibility, depending on the strength of this interaction; if moderate can lead to miscibility, if the interaction is strong then the phase separation is associative, characterized by one concentrated phase that can be a viscous liquid, gel or precipitate, in equilibrium with a dilute phase.

It is already known that DNA interacts with oppositely charged amphiphiles in an associative manner(*38*). Associative phase behavior occurs when there is a strong attraction between two components, therefore they generally present opposite charges. A common phase diagram representing the associative phase behavior between two polymers of oppositely charges in a solvent is depicted in Figure 9. The tie-lines running to the solvent corner, visualized in the figure, express the phase separation into one dilute phase, with the composition closer to the solvent corner, and one concentrated, in both polymers, with the composition opposite to the corner.

The phenomenon of formation of gel particles, due to associative phase separation, through the interaction at the interface water / water of two oppositely charged polyelectrolytes was the basis of this work.

1.6 Nano-Technology

An exciting revolution in health care and medical technology looms large on the horizon. Yet the agents of change will be microscopically small, future products of a new discipline known as nano- technology.

Nanotechnology involves the manipulation of matter at the molecular scale and has the potential to fundamentally alter the way people live, by providing new drug delivery systems, faster and cheaper manufacturing processes, cleaner and more efficient energy generation, new materials, clean water and the next generation of computing devices.

But what is the real meaning of the word nano? In this context, the word nano is not the smallest thing on the planet or in space. Protons, neurons, quarks, leptons and neutrinos are considered as the family of electrons, out of which quarks and leptons are the smallest known particles. A nanometre (nm) is one thousand millionth of a meter. Just as example, the size of a flea is 1000000 nm, the width of a bacterium is 1300nm, the diameter of a ribosome 20nm and DNA chain approximately 2.5 nm (see Figure 10).

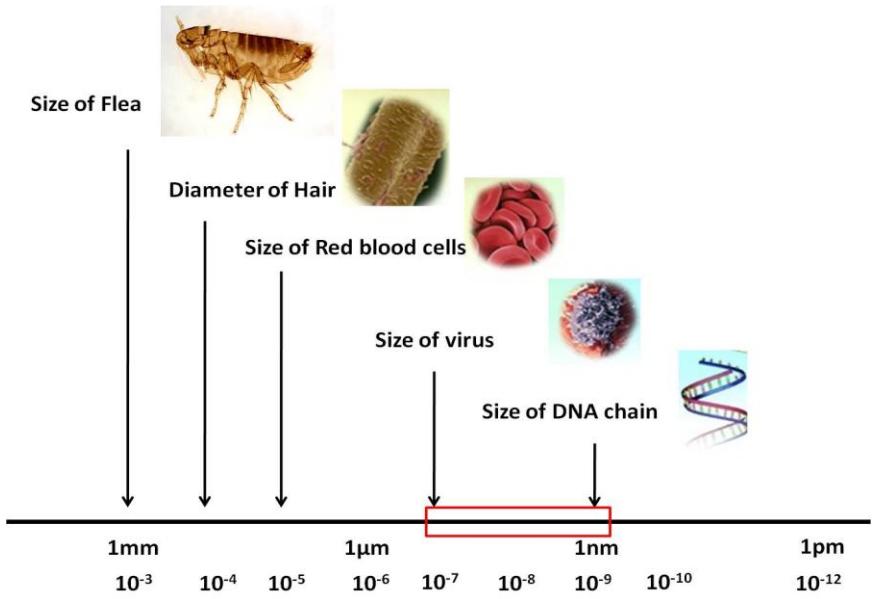

Figure 10 - The scale of things: length scale showing the nanometre in context. The nanoscale is considered to consist of entities in the range 1 to several hundred nm, as highlighted in the red box(adapted from reference (*40*)).

We can define nanotechnology as the engineering of functional systems at the molecular scale, which makes possible to build machines on the scale of human cells or create materials and structures from the bottom up with novel properties. Therefore is somehow easy to understand the outstanding potential that nanoscience has in so many areas from textile, defence and security, energy, food and agriculture, to the focus of this thesis: medicine and drug delivery.

1.6.1 Nanomedicine: a new field

A growing interest of nanotechnology in medical applications, has led to the emergence of a new field called nanomedicine(*41*).

Nanomedicine uses nanosized tools for the diagnosis, prevention and treatment of disease and to gain understanding of the complex underlying pathophysiology of disease. The ultimate goal is to improve the quality of life. The aim of nanomedicine may be broadly defined as the comprehensive monitoring, repairing and improvement of all human biological systems, working from the molecular level using engineered devices and nanostructures to achieve medical benefit (*42*).

For example, a typical cancer cell, is approximately 20000 nm in diameter, a bacteria 1000nm, while a quantum dot is about the same size as a small protein (<10 nm) and some viruses measure less than 100 nm (Figure 11).

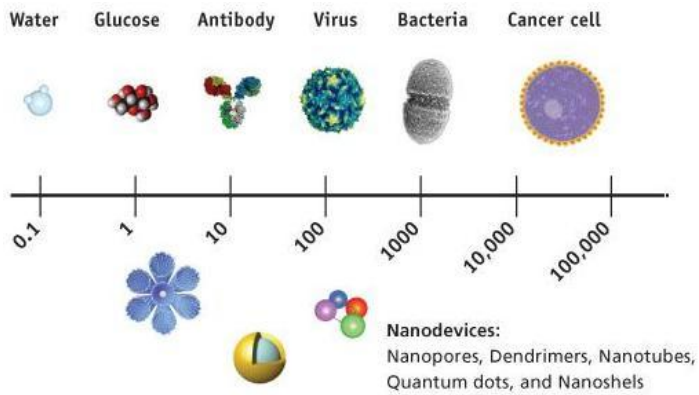

Figure 11 - Development of nanotechnology. Nanometre scale.

These devices could remove obstructions in the circulatory system, kill cancer cells, or take over the function of subcellular organelles. Just as today the artificial heart has been developed, so in the future, perhaps artificial mitochondrion would be developed. Nanomedicine offers the prospect of powerful new tools for the treatment of human diseases and the augmentation of human biological systems.

Targeted drug delivery is the most important goal of pharmaceutical research and development. In this context drug targeting is defined in the broadest sense, that is, to optimize a drug's therapeutic release by strictly localizing its pharmacological activity to the site or organ of action, and definitely this may be the most profitable application of nanotechnology in medicine, and even generally, over the next two decades.

1.6.2 Nanoparticles: nanodevices for drug delivery

Nanoparticles for the purpose of drug delivery are defined as submicron (<1μm) colloidal particles. This definition includes nanospheres in which the drug is adsorbed, dissolved, or dispersed throughout the matrix and nanocapsules in which the drug is confined to an aqueous or oily core surrounded by a shell-like wall. Alternatively, the drug can be covalently attached to the surface or into the matrix. Nowadays is possible to find many different kind of nanoparticles, ranging from biocompatible and biodegradable materials such as solid lipids and polymers, either natural (e.g., gelatin, albumin) or synthetic (e.g., polystyrene), to gold, mesoporous silica, magnetic nanoparticles, quantum dots, etc. (see Figure 12).

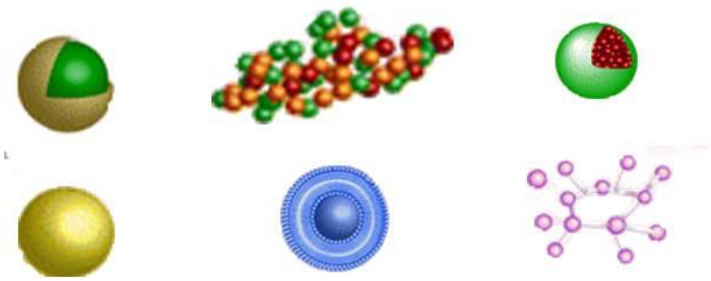

Figure 12 - Different types of nanoparticles; the surface of a nanoparticle can be functionalized with hydrophilic polymers, targeting molecules (e.g., antibodies), drugs and imaging contrast agents for diagnostics. The interior core can be solid (e.g., quantum dots), liquid (e.g., liposomes) or contain an encapsulated drug.

The following are among the important technological advantages of nanoparticles as drug carriers: high stability (i.e. long shelf life); high carrier capacity (i.e. many drug molecules can be incorporated in the particle matrix); feasibility of incorporation of both hydrophilic and hydrophobic substances; and feasibility of variable routes of administration, including oral administration and inhalation.

The efficacy of many drugs is often limited by their potential to reach the site of therapeutic action. In most cases (conventional dosage forms), only a small amount of administered dose reaches the target site, while the majority of the drug distributes throughout the rest of the body in accordance with its physicochemical and biochemical properties. Therefore, developing a drug delivery system that optimizes the pharmaceutical action of a drug while reducing its toxic side effects *in vivo* is a challenging task (*43*).

One approach is the use of colloidal drug carriers that can provide site specific or targeted drug delivery combined with optimal drug release profiles.

The idea of using submicron drug delivery systems for drug targeting was conceived and developed after Paul Ehrlich originally proposed the idea of tiny drug-loaded magic bullets over a hundred year ago.

Among these carriers, liposomes and micro/nanoparticles have been the most extensively investigated. Liposomes present some technological limitations including poor reproducibility and stability, and low drug entrapment efficiency.

Nevertheless, several low molecular weight drugs are now commercially available which employ this technology. Polymeric nanoparticles, which possess a better reproducibility and stability profiles than liposomes, have been proposed as alternative drug carriers that overcome many of these problems.

Chapter2.

Discussion of results

2.1Chapter Introduction

In this chapter the results obtained during this project will be reported and discussed. Initially, it was necessary to find out what were the most favorable conditions, in terms of viscosity and concentration, to obtain DNA gel particles. The next step went through an approach about the physicochemical properties of this system. What kind of morphology do these particles present? What is the structure and the degree of complexation of the drops of DNA, when in contact with the cationic polyelectrolyte solution? How much of DNA can be encapsulated in this system and how long is it possible to have stable particles? What is the charge of these particles? Is it possible to move this system to the nanoscale range? Are these particles cytotoxic? These are some of the questions that came along over this journey through the world of DNA and Chitosan Lactate, through nanoparticles and gene delivery. The biggest purpose of this thesis is to find a path to prove that Chitosan Lactate is a safe and efficient gene carrier.

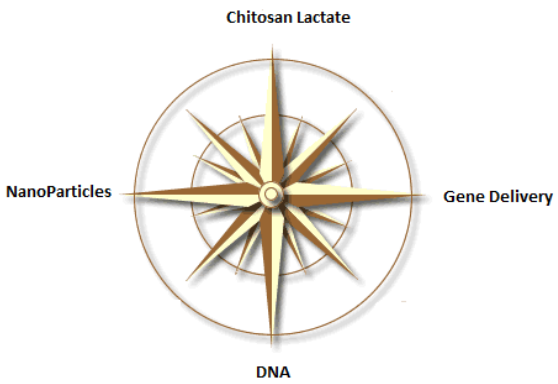

2.2Complexation

Besides the mechanism of complexation, the chemical and biochemical properties of DNA-Chitosan complexes also depend on the chitosan cationic charge density and valence, the former being influenced for the chitosan degree of acetylation and pH of the medium and being proportional to the chitosan molecular weight(*44-45*).

It is known that high charge density of chitosan at pH below the pKa results beneficial for complexes preparation and also that its low charge density at pH 7.4 may contribute to a low complex citotoxicity and may facilitate the intacellular release of DNA from the complex after its endocytotic cellular uptake (*46*).

Some derivative including glucosylated (*47-48*), pegylated (*49-50*)and trimethylated chitosans (*49, 51*) have also been tried but the criteria and strategies for the design of efficient chitosan gene delivery systems remain inconclusive. But what happens with lactate?

In order to form DNA gel particles, the DNA solution need to have some viscosity due to the compromise between the droplet dissociation and the complexation of the cationic agent. The biggest premise is that to have gel particles, it is need to have a localized associative phase separation, otherwise two separated phases will form. Former works in the group, done with CTAB, cetyl trimethylammonium bromide, reveal that the concentration of DNA should be around 60mM, as it can be seen in Figure 13. Despite the fact that this cationic agent is totally different than CL, since CTAB is a cationic surfactant, it can help us identifying the region where the DNA drop have an appropriate viscosity for the DNA gel particle formation.

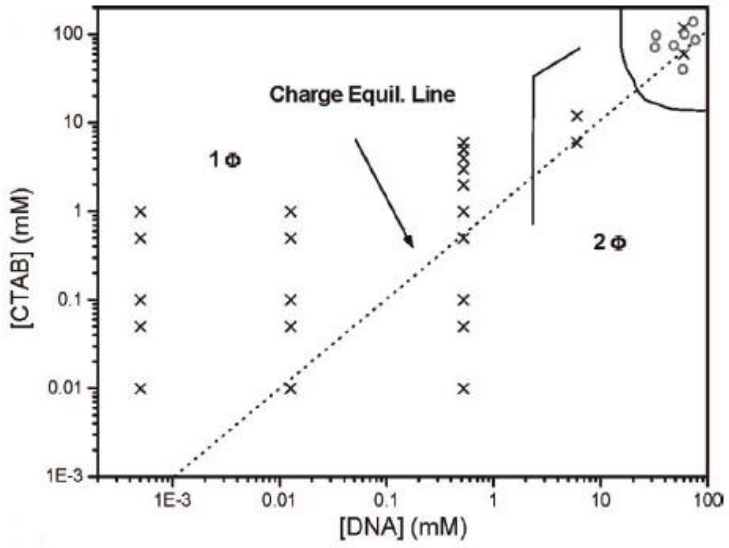

Figure 13 - Formation of DNA Gel Particles. Phase-map of the CTAB/dsDNA/water mixture at 25^{0}C, where 1Φ and 2Φ indicate the one and two phase regions, respectively (x) studied compositions and (o) area where gel particles were observed. (adapted from reference (*52*))

Once a solution of 60mM of DNA gave good results for experiments with CTAB and it´s known that the viscosity of the drop, play a central role in the complexation process, some experiments with CL were performed. As was mentioned above, the choice of this concentration of DNA reflects the fact that it produces high viscosity solutions, which makes it a convenient system for the preparation of stable DNA gel particles (*53-54*).

The formation of DNA gel particles was studied using mixture of dsDNA and CL, the last with concentration between 1 and 6 mM. For all cases DNA´s concentration was 60mM.

For lower concentrations (<1mM) of CL there was not formation of particles, only two phases separated. For higher concentrations that the selected range

(>6) that is possible to see in Figure 14, at the end of 2 hours, particles were too shrunken.

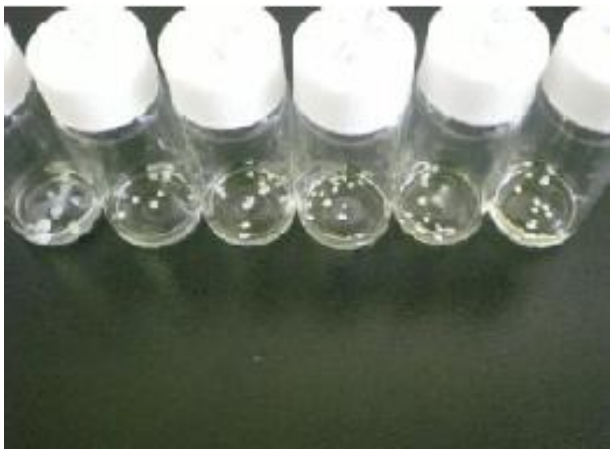

Figure 14 - DNA gel particles.

Additional information about the degree of complexation as well as changes in the particle size during the particle formation process has been obtained by continuously monitoring these systems by a video camera (see Figure 15). The study reveals that particles suffer a higher degree of complexation in the first minutes of interaction, due to more exposal charges between the DNA and the CL. Higher concentration of CL allows the formation of smaller particles (See Figure 15 and 16). The equilibration time was 90 min.

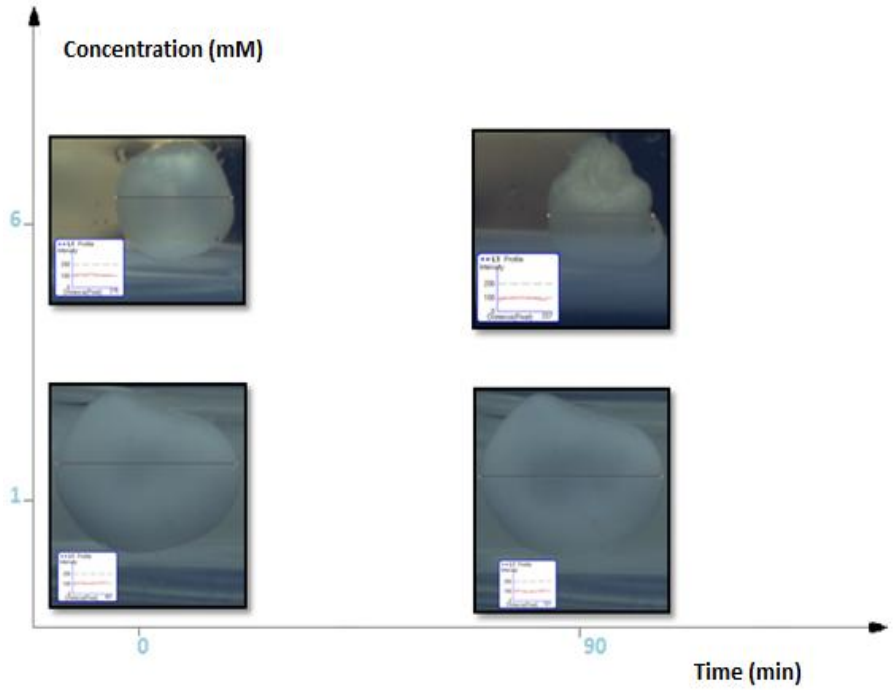

Figure 15 –Influence of the chitosan concentration and time on the complexation process.

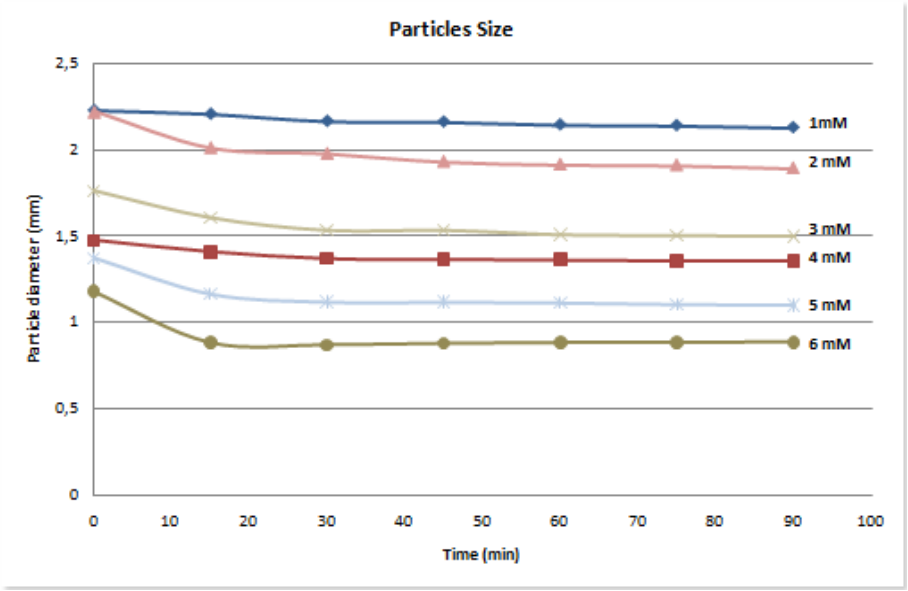

Figure 16 – Graphic representation of Particles size in function of time.

Particles exhibited a high tendency to aggregate, showing a bigger degree of instability for the lowest concentration. As the ratio charge (See Chapter 4, section 4.4.3) between DNA and CL decreases, well defined particles were formed.

In fact, the size of these gel particles, as well their opacity can indicate the degree of complexation suffered by the drop of DNA. Particles exhibited smaller sizes than 2.5mm and the sizes decreased as the concentration of CL increased. Changes in opacity reveal the neutralization of charges during the complexation time and it is increased with the time.

The size of the resulting particles reflects the size of the parent drop but also the concentration of CL.

Keep in mind:

- Particles size and opacity are indicative of the complexation´s degrees, and are a function of the concentration of CL.
- Besides the known drop size factor, the concentration of the cationic polyelectrolyte plays a crucial role in the final size of the particles

2.3 Morphology and Structure

The best way to confirm the type of complexation and the kind of morphology and structure the particles reveals, goes through measures of fluorescence, since this technique allows verifying if the secondary structure of DNA is kept during the encapsulation and studying the morphology of the particles formed, establishing the degree of complexation suffered by the drop of DNA.

It is possible to differentiate between core-shell particles, i.e., particles where the complexation, discussed in section 2.2, only reaches the surface of the droplet and solid particles, where CL can penetrate the entire droplet. These two different morphologies can be more noticeable in Figure 17.

Figure 17 – Schematic representation of a) Core-shell particle; b) solid particle.

The integrity and the conformational state of DNA in the particles have been determined using the fluorescent probe AO. As described in chapter 4, it can be seen that the complex AO-dsDNA has a green emission while the AO-ssDNA one has a red emission. This is a key fact for this evaluation, since if occurs denaturation of DNA, we would see red on the images of Figure 18. The absence of red emission confirms that the secondary structure of DNA is preserved.

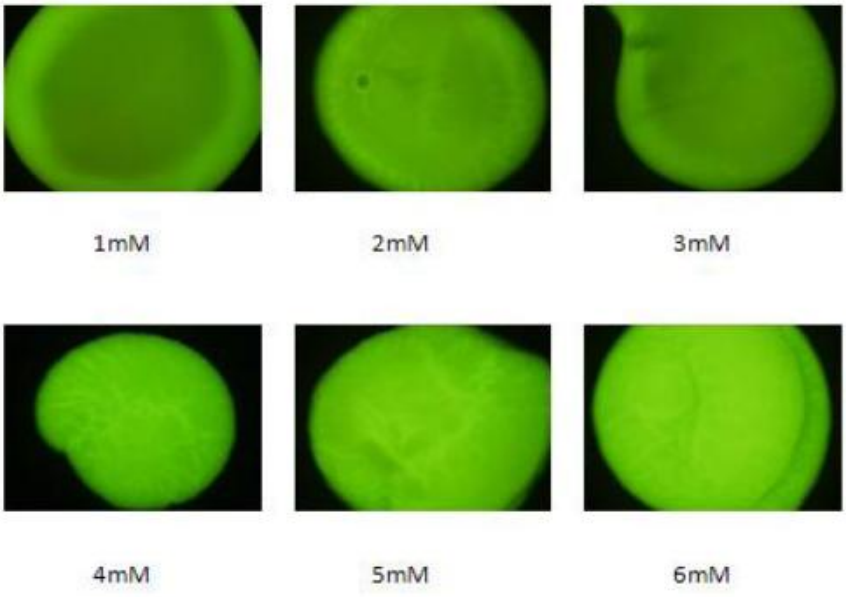

Figure 18 – CL/dsDNA gel particles viewed by FM with filter MNIBA3 (excitation 470nm and dichromatic mirror of 505nm).

One characteristic of this particular CL is that it appears to show auto fluorescence. It is difficult to find references of this fact for other chitosans, but the results that were obtained appoint on this direction. Thus, analyzing the solid CL by means of fluorescence microscopy, it is possible to see that, without adding any dye is possible to have fluorescence using two different excitation filters sets. According to Figure 19, using the filter with an excitation wavelength between 470 and 495 nm, CL has a green emission, using the one with a wavelength between 360 and 370 nm, CL has a blue emission.

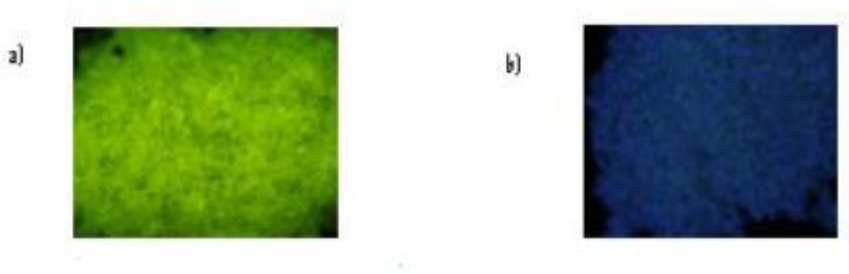

Figure 19 – Solid CL viewed by FM with two different excitation wavelengths filters: a) 470-495nm; b) 360-370nm.

This feature is of particular importance since it allows identifying the presence of CL and DNA simultaneously by fluorescence microscopy.

Using a different filter-set, it is also visible that, for concentrations of CL above 4mM, the appearance of a blue emission is increased, sign of an excess of CL (Figure 20). This allows us to set a barrier between the different types of morphology. From concentration of CL from 1 to 3mM core-shell particles have been obtained. For higher concentration of CL, solid particles have been obtained.

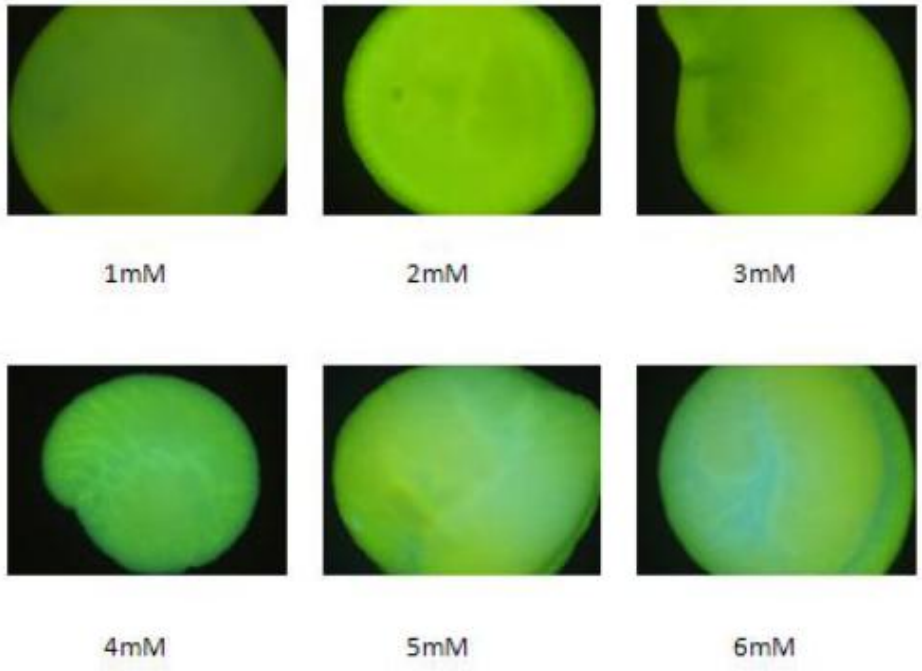

Figure 20 – CL/dsDNA gel particles viewed by FM with filter U-MNU2 (excitation 370nm and dichromatic mirror of 400nm).

Our results seem to be in agreement with those from Lapitsky et al (*53-54*), where they suggest that, the structure of particles is ruled by the composition of solution and by the method of preparation, while the stability of them concerns with phase behavior.

In addition, SEM has become an invaluable technique in the characterization of particle´s morphology. Although the procedure described in chapter4, would cause some deformation in the shape and arrangement, the nature of cationic agent would be the most important factor in the diverse morphologies of the obtained DNA gel particles.

One serious disadvantage of this technique, is the risk of changes in particle´s properties during drying and contrasting of the sample. In the present study, which used freeze-drying and subsequent Auto-shadowing as method

preparation, shrinking of particles during drying was a problem that affects our results and so we were unable to prove the real barrier between the core-shell and solid particles.

Nevertheless, is possible to obtain data from SEM that confirm the shell of the particle and the presence of DNA inside the particle and compare this image to one from previous studies done with CTAB. The DNA encapsulated with the surfactant is much more visible and seems not to collapse into the shell of the particle (See Figure 21).

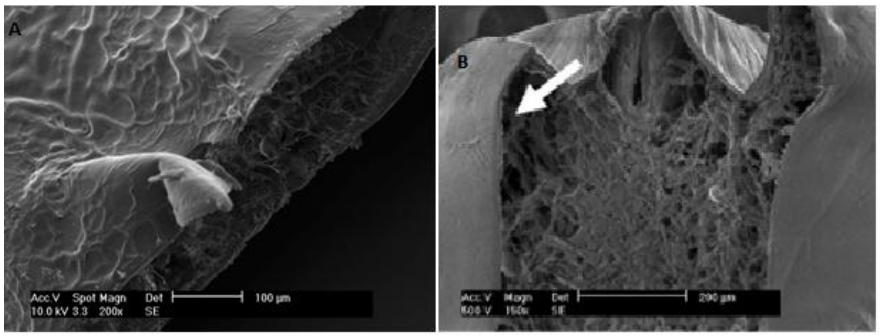

Figure 21 – a) CL/DNA gel Particle (2mM) visualized by SEM; b) CTAB/DNA gel Particle visualized by SEM.

Keep in mind:

- The secondary structure of DNA is kept.
- Chitosan Lactate can be visualized when is in excess by Fluorescence Microscopy.
- It´s possible to find a tendency that show that for concentration of Chitosan Lactate superior than 4mM, a transition from core-shell particles to solid particles takes place.

2.4 DNA complexation and release

Although is known that chitosan molecules are able to complex DNA, the properties of DNA-chitosan complexes depend strongly on the structure of chitosans(*16*). In order to find the kinetics of release and the encapsulation´s degree of the DNA-chitosan lactate based particles were performed some measures of UV-VIS spectroscopy. We are also interested in examine the particles stability.

The DNA released on the media was monitored at defined time intervals by UV-Visible measurement at 260 nm. The representation of cumulative DNA released, as a function of time, is showed in Figure 22. It´s visible that, for higher concentrations of CL, the release of DNA is slower comparing with that observed for more diluted systems. However, after 24hours almost all DNA included in the particles is released in the solution. The total dissolution of the particles was observed after 48 hours.

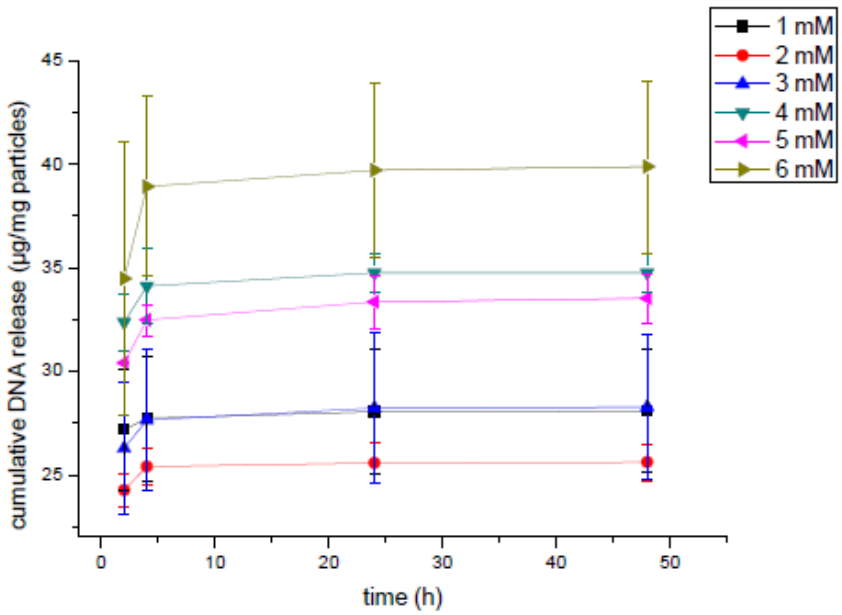

Figure 22 – Graphic representation of the released dsDNA quantity in function of time, for different CL concentrations.

In order to have a better idea of the speed of DNA release on the media the percentage of released DNA as a function of time has been plotted (see Figure23).

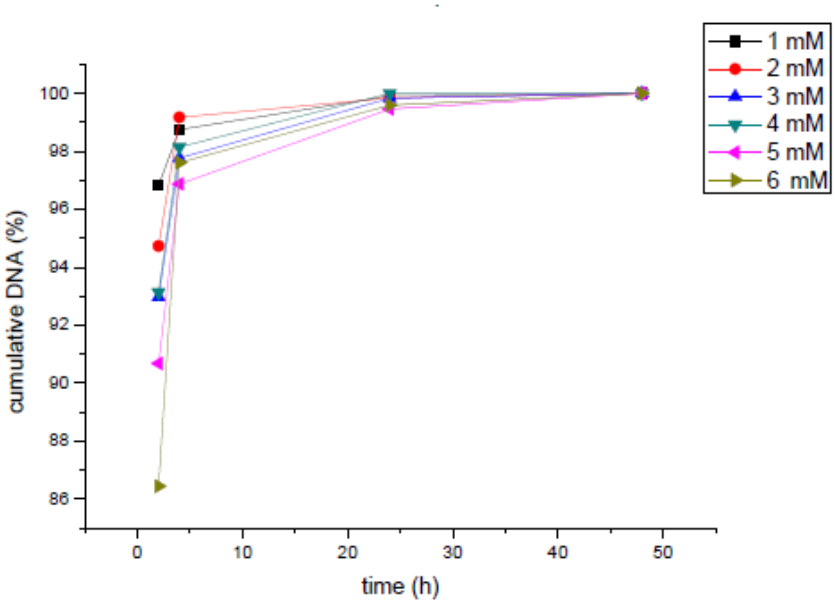

Figure 23 – Graphic representation of the percentage of released DNA, for the different CL concentrations.

Although the observed DNA release is a quite fast process, it is possible to observe the influence of the chitosan concentration in the solutions in which the particle formation takes place: the lower the chitosan concentration the faster the DNA release.

In addition, the degree of encapsulation has been calculated through the Loading Capacity value (LC):

$$LC\ (\%) = \frac{total\ amount\ of\ DNA - free\ DNA}{Particle's\ weight}$$

that relates the quantity of released DNA on the particles in function of their weight.

The degree of encapsulation of the different systems is shown in Figure 24:

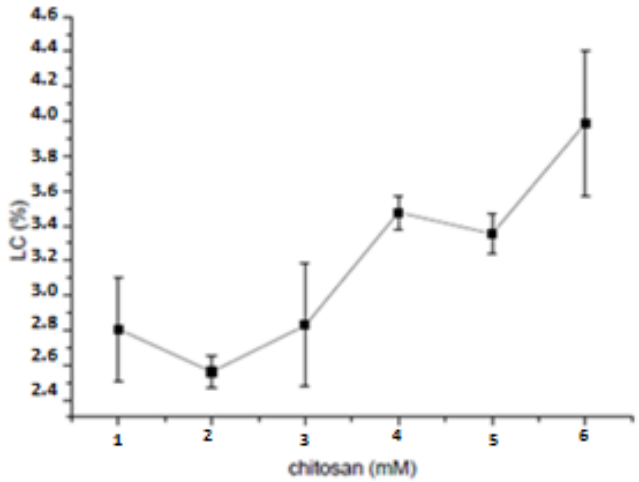

Figure 24 – Graphic representation of dsDNA Loading Capacities for different concentrations of CL.

As expected, it is possible to see that for higher concentrations of CL more DNA is encapsulated. This parameter also shows that, the capacity of chitosan lactate to encapsulate DNA is quite high and that aspect could be a promising indication of CL as an effective gene carrier.

Further, experiments of electrophoresis in agarose gel have been carried out, in an attempt to evaluate the stability of the different CL-dsDNA particles on the electric field. As is possible to see in Figure 25, the amount of DNA that migrates to the positive electrode is very similar for the different particle systems. This fact is in agreement with the little stability of these particles, which when subjected to the applied potential are torn apart. Interestingly, it is possible to observe the migration of CL to the negative electrode. This experiment allows us to confirm that for a concentration of chitosan higher than 4 mM, an excess

of CL is present on the particles. These results are in agreement with the FM studies described above.

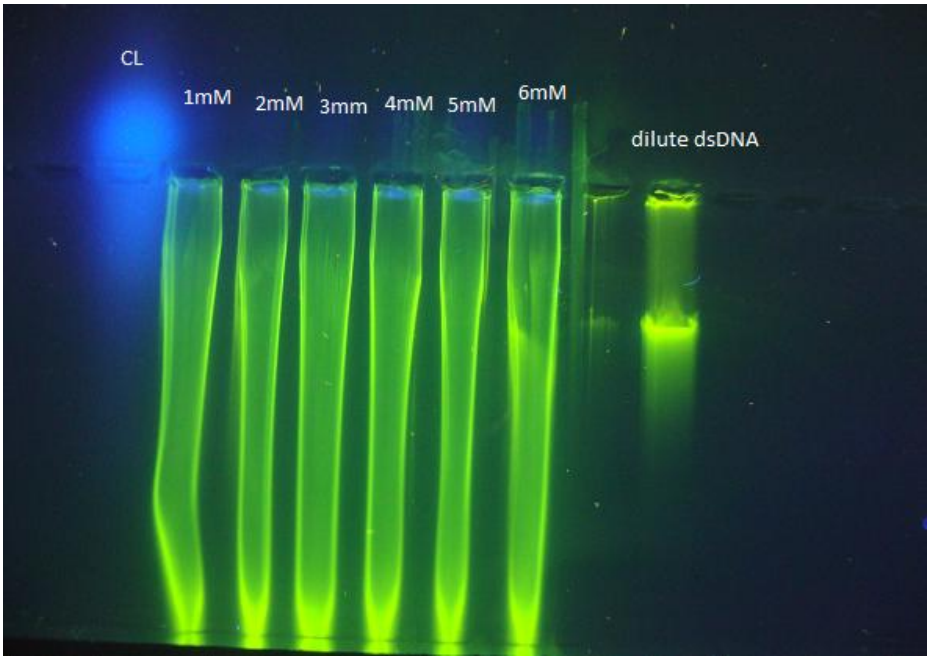

Figure 25 – CL, dsDNA and CL/dsDNA particles behavior on an experiment of electrophoresis in agarose gel.

2.4.1The ss-DNA problem

Previous studies in the group reveal that the interaction between ssDNA and cationic entities, most specifically surfactants like CTAB, was higher that with ds-DNA (*52*). So, this kind of tendency was expected to happen also in our system.

CL-ssDNA particles have been prepared in the same interval of CL concentration that in the case of the native nucleic acid. However, visual inspections, as well as FM studies, demonstrate that the system CL/ssDNA is

highly instable. Once the transition between concentrations seemed to be more drastic, we introduced two more concentrations: 1.5 and 2.5 mM.

Figure 26 shows representative FM images of the CL-ssDNA gel particles.

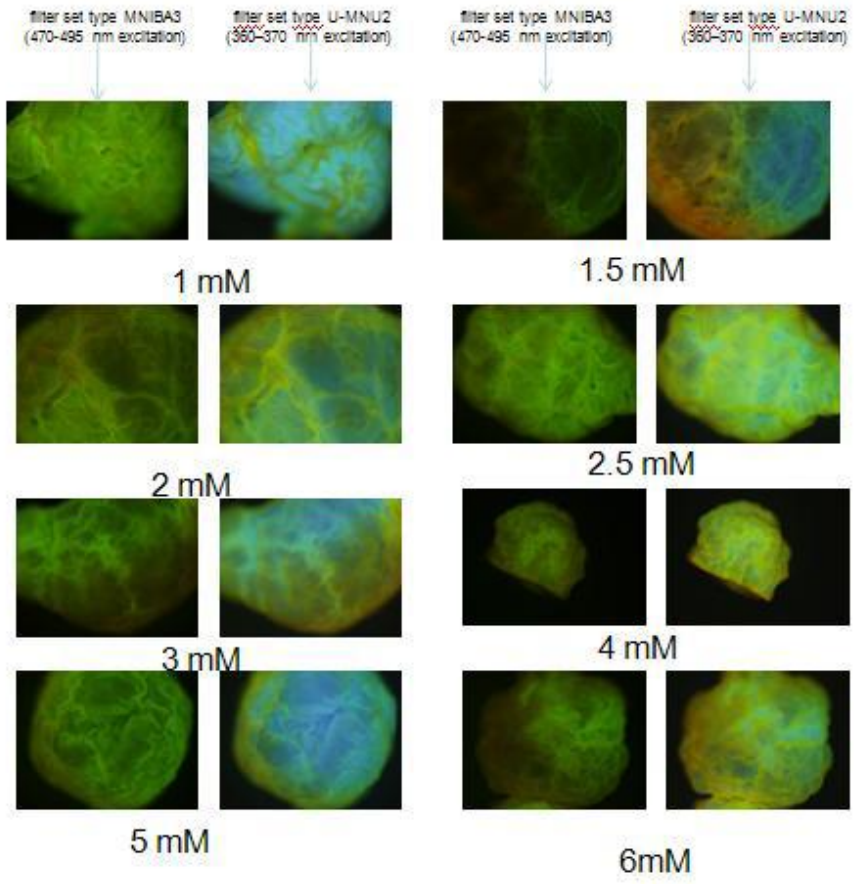

Figure 26 – CL/ssDNA gel particles visualized by FM with both filters.

In fact, it is more difficult to see a transition between the core-shell type of particles and the solid ones. There is a high overlap of colours, due to different emissions sources.

Once CL-ssDNA particles were very unstable (they are completely disrupted at the end of the equilibration time), the kinetics of DNA release have not been determined. However, Loading Capacity (LC) values were calculated and plotted (Figure 27). Although there is no a clear trend on the LC values, it is interesting to note how the LC on the CL-dsDNA particles can be twice the observed in the case of CL-ssDNA particles.

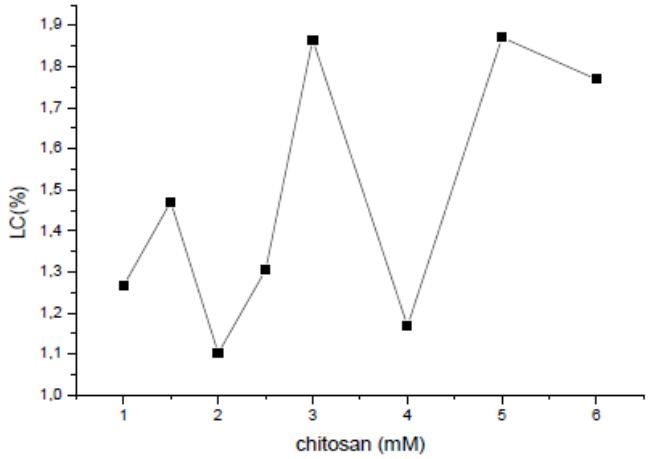

Figure 27 – Loading Capacities for the CL/ssDNA system.

Thus, what kind of differences is responsible for the instability of particles when ssDNA is used?

By visual inspection, the apparent viscosity of a 60 mM concentration of ss-DNA solution is higher than in the case of dsDNA. This fact could difficult the drop wise addition and the parent drop, which are factors that can influence the particle formation. In this case, we obtain deformed drops with a viscosity superior than expected, interacting with the same solution of chitosan lactate. As a consequence, unstable particles could be obtained. In that point, there are two questions that need to be answered. First of all, is why the viscosity increases

with the denaturation of DNA, when is mentioned in literature (*11*)that should decrease. When DNA denatures, the two strands separate and each single strand is free to adopt different conformations, in a form of a random coil. This form has a lower intrinsic viscosity than the double stranded DNA.

But what if, this property happens only for dilute concentrations of DNA? To answer this question, were measure solutions of DNA, both single and double stranded, with a range of defined concentration and subjected them to shear forces, in order to evaluate the viscosity of solutions. Figures 28 and 29 show the obtained results.

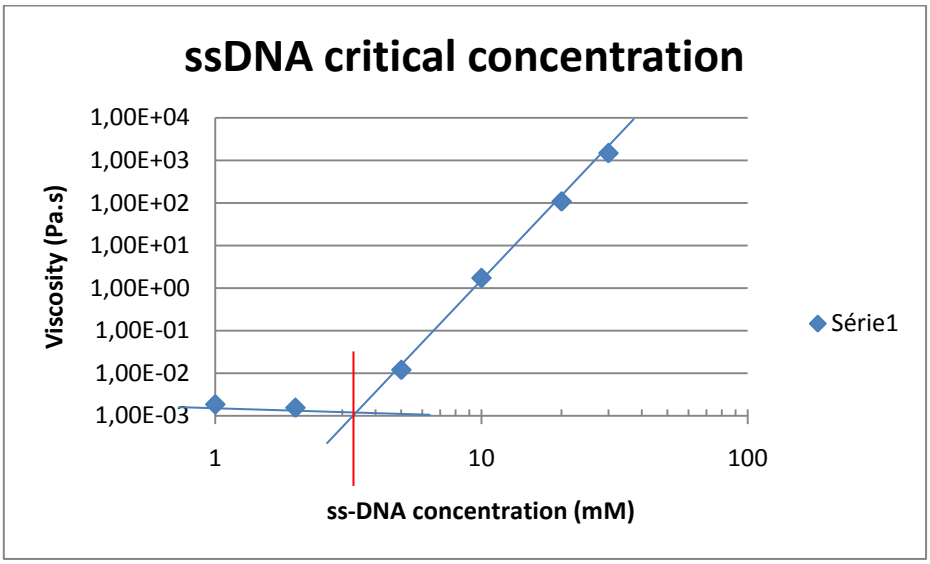

Figure 28 – ssDNA viscosity in function of its concentration.

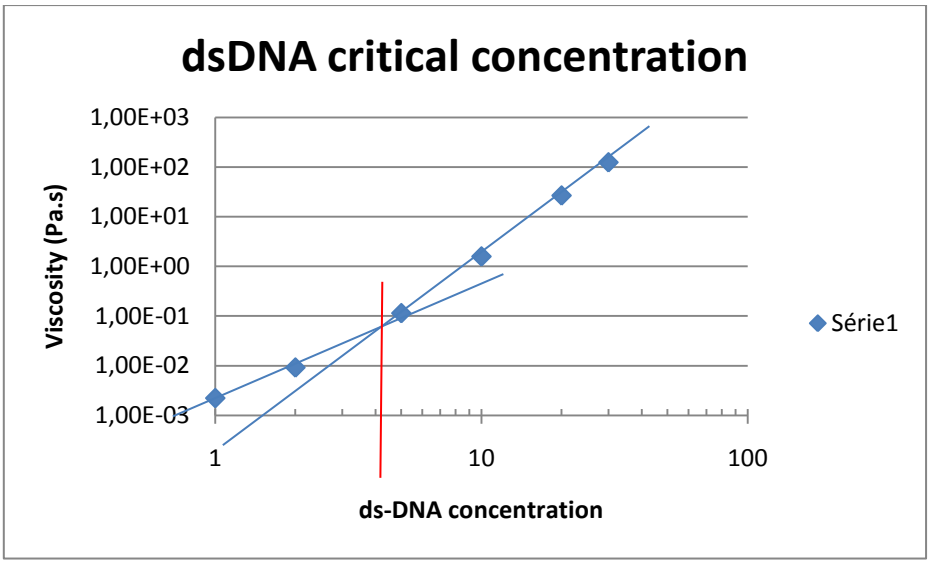

Figure 29 – dsDNA viscosity in function of its concentration.

From these figures is possible to define that the critical concentration of ssDNA (≈ 3.5mM) is lower than the one for dsDNA (≈ 4.2mM). From solutions of DNA of 2mM the viscosity of ss is 1.55 E^{-3} Pa.s, while in the ds state is 9.16 E^{-3} Pa.s. For concentrations around 10mM, we can see an inversion of this behavior and from those values forward the viscosity of ds-DNA is lower than the viscosity of ssDNA. For example, for a concentration of 30mM the ss viscosity value is 1.48 E^{3} while for the ds is 1.25 E^{2}, i.e., an order of magnitude less viscous. With this study, we can conclude that, for the range of concentrations that was used in this work, the ssDNA is more viscous than dsDNA, and this fact have a particular negative impact on the formation and stability of the CL/ssDNA gel particles.

Keep in mind:

- DNA is totally released from CL-dsDNA particles after 48 h.
- CL-dsDNA particles show LC values around 4%.

- Differences in viscosity of ssDNA and dsDNA solution could explain the instability of CL-ssDNA particles for the same range of CL concentrations.

2.5NanoParticles

Although the molecular details of the mechanism by which cationic carriers mediate DNA delivery are still poorly understood, current evidence supports the hypothesis that the cationic entity-DNA complexes enter cells by mean of endocytosis. Often, the particles size ranges from 100 nm to higher than 1um and, evidently, the efficiency of cellular uptake and subsequent intracellular transfection may well depend on particle size (*55*).

To address the problem of the size of the obtained DNA gel particles, we speculated that aerosol techniques at micron level size. Delivery of gene formulations via aerosols is a relatively new field, which is less than a decade old. However, in this short period of time significant developments in aerosol delivery systems and vectors have resulted in major advances toward potential applications for various pulmonary diseases. Air-jet and ultrasonic nebulizations are the two predominant methods utilized therapeutically to aerosolize drug solutions. Air-jet nebulizers operate with compressed air, transporting liquid through nozzles creating small aerosol droplets, whereas ultrasonic nebulizers use the piezoelectric effect to generate high frequency acoustic energy which generates aerosol droplets by cavitation. Both types of nebulizers offer various advantages and disadvantages. Air-jet nebulization can affect gene carrier systems as a result of the high shear forces applied during nebulization. Ultrasonic energy is notorious for altering or damaging some aerosolized drug substances(*56*). Furthermore, ultrasonic nebulizers are usually more expensive and have not yet

been investigated for the aerosolization of gene delivery systems based on cationic polymers. To date, only air-jet nebulizers have been used in inhalative gene therapy studies(*57*).

Of major interest in the characterization of submicron particles is the size, as it can give useful information as to whether the nebulisation process was successful. It was also shown that particle size can influence body distribution(*58*). In addition, connected with the size is the polydispersity index. A monomodal and narrow size distribution should be the aim of nanoparticle preparation, to ensure uniform distribution behaviour of the particles upon administration. Visualization of these systems, however, remains an invaluable tool to get a better understanding of the colloidal systems.

The first step to create these nanoparticles was to find a concentration of DNA that could be able to form them. Due to limitations of the nebulizer the viscosity of the corresponding DNA had to be low. According to some studies proceeded by the group (*59*) it was found that a concentration of 5mM solution of DNA was the highest one that is possible to use in order to be nebulized properly. Nanoparticles were prepared at a fixed ratio (r) of 1 where:

$$r = \frac{[DNA]}{[CL]}$$

The obtained nanoparticles were initially analysed using some fluorescence microscopy measures (See Figure 30).

Figure 30 - CL /dsDNA NanoParticles viewed by FM.

Actually, analyzing the Figure 30, we are able to say that, the particles were formed and the secondary structure of DNA was kept.

What about the size distribution of the particles?

As was noted in the introduction of this section this is an important factor that needs to be taken into account. Thus, further studies by Photon Correlation Microscopy (PCS) were carried out, in order to give us some information about the actual size and polydispersion of the obtained particles.

As we can see in Figure 31, particles were obtained with a broad dispersed population.

90.0° Unimodal Distribution

Unimodal Results Summary

Rept#.	Mean (nm)	P.I.	Diff.Coef (m^2/s)	Counts/s	Baseline Error	Overflow
Rept.1	618.4	1.047	7.93e-13	7.71e+04	11.42%	296
Rept.2	788.8	1.266	6.22e-13	7.54e+04	14.10%	18
Average	703.6 ± 85.20	1.156 ± 0.110				

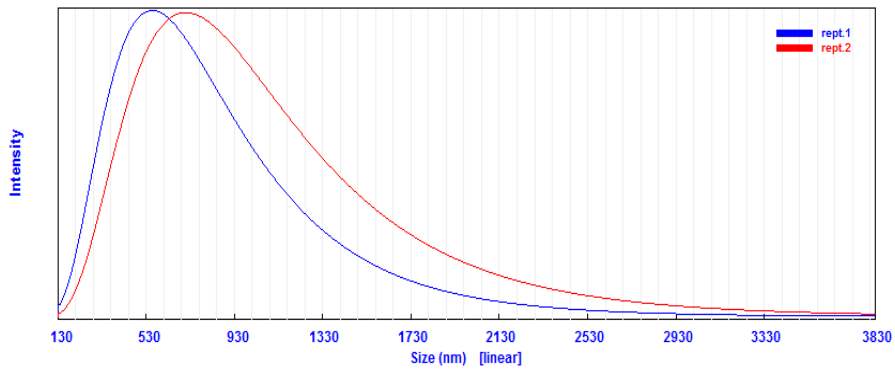

Figure 31 - Size distribution of 5mM CL/dsDNA NanoParticles.

The existence of more than one population was identified, when the measurement was performed using a multimodal device (see Figure 32).

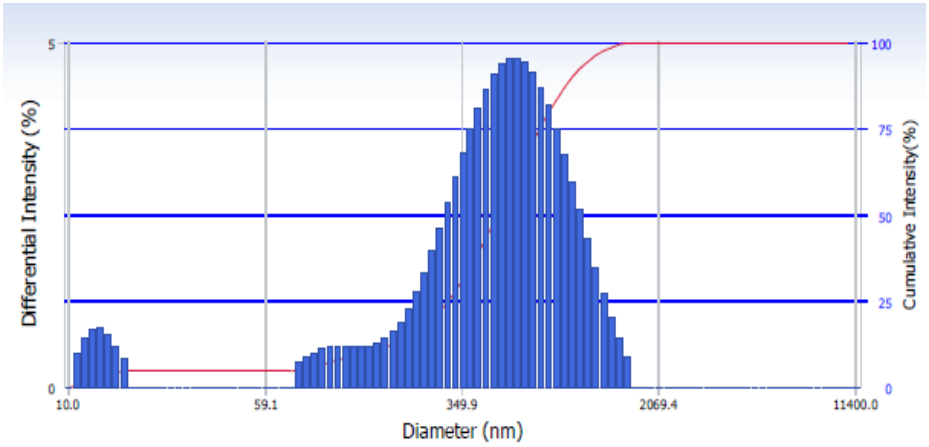

Figure 32 - Size distribution of 5mM CL/dsDNA NanoParticles measured by a multimodal PCS.

We can distinguish between 3 populations: one about 20 nm, one with approx. 150nm, and a large one with a mean value of 623.4 nm, which corresponds with the size of chitosan lactate

An initial study using a 30,000 MWCO cut off concentrator demonstrated that this procedure (centrifugation + filtration) is useful to discriminate between big particles (around 2.5 µm) and smaller particles (around 1 µm) that can be observed by FM. Figure 33 show the existence of particles and conservation of DNA secondary structure on both down and upper part of the concentrator.

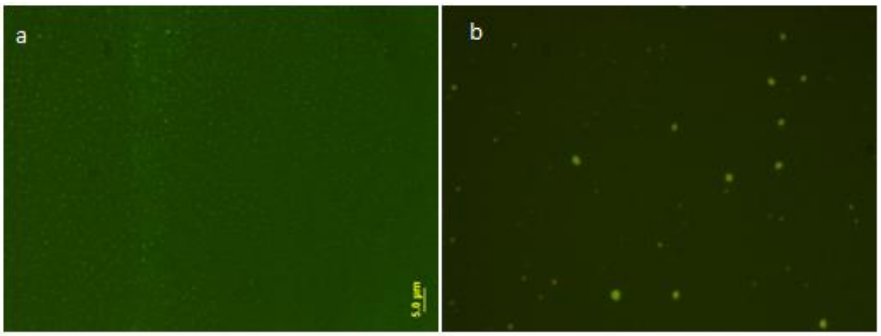

Figure 33 – FM images of NanoParticles after concentrated with the 30, 000 MWCO concentrator. a)down part of concentrator; b) upper part of concentrator.

PCS studies of the down part showed that besides the fact that particles are more refined now, we still have a considerable dispersion of sizes. In addition, CL was not removed from the solution (See Figure 34).

90.0° Unimodal Distribution

Unimodal Results Summary

Rept#.	Mean (nm)	P.I.	Diff.Coef (m^2/s)	Counts/s	Baseline Error	Overflow
Rept.2	504.3	0.800	9.73e-13	4.29e+04	3.90%	10
Rept.4	482.5	0.962	1.02e-12	4.24e+04	1.65%	0
Rept.5	534.5	1.046	9.18e-13	4.41e+04	2.10%	0
Average	507.1 ± 79.22	0.936 ± 0.136				

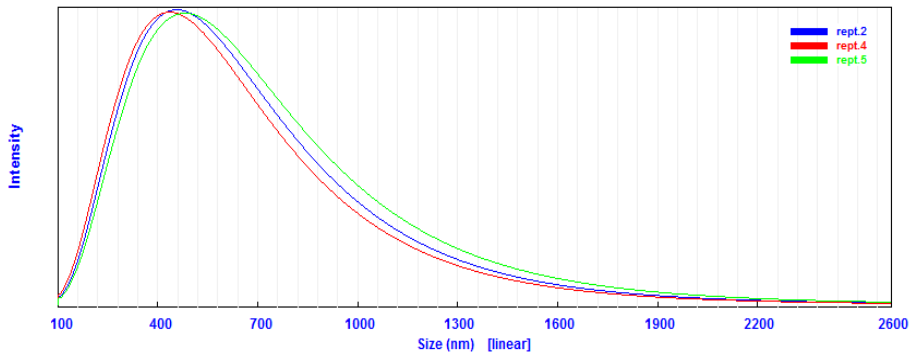

Figure 34 - Size distribution of NanoParticles after filtration with a 30,000 MWCO concentrator.

Further studies were carried out, using a concentrator, with a smaller cut off size. Considering that chitosan lactate has a molecular weight around 5,000 kDa, a 3,000 MWCO concentrator was chosen. Figure 35 shows a representative image of the total dispersion and the upper and bottom fractions obtained after centrifugation.

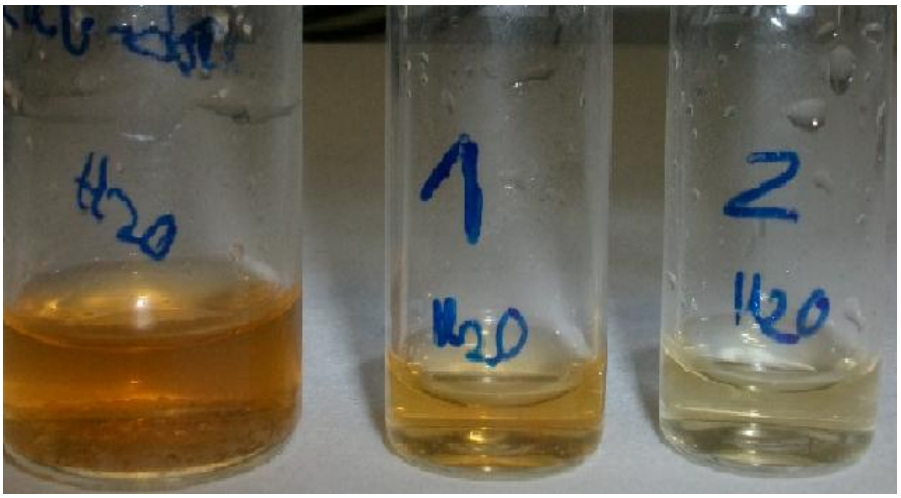

Figure 35 – Dispersions of CL/ds-DNA NanoParticles. From the left to right represent the solution obtained with the nebulizer, the next one represent the upper part collected from the concentrator and the last, the down part.

The solutions collected in the down part of the concentrator have a notorious discoloration indicating that that CL in excess was removed from the solution.

All three dispersion were analyzed with a Zetasizer in terms of size distribution and polydispersity (See Figure 36 and 37).

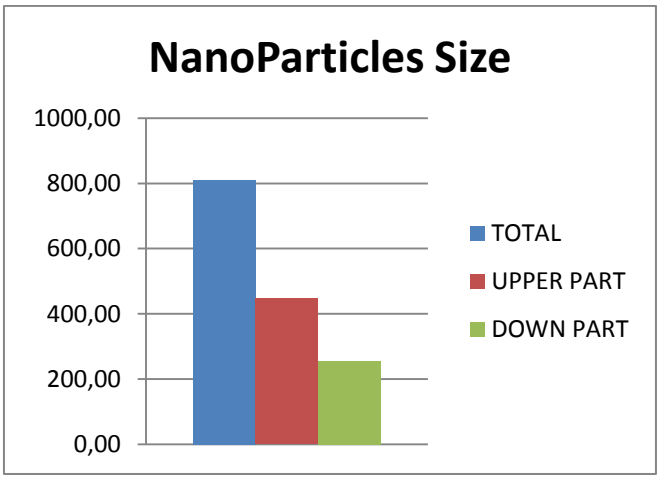

Figure 36 - Graphic representation of NanoParticles sizes before (total) and after filtration (upper and down parts) with a 3,000 MWCO.

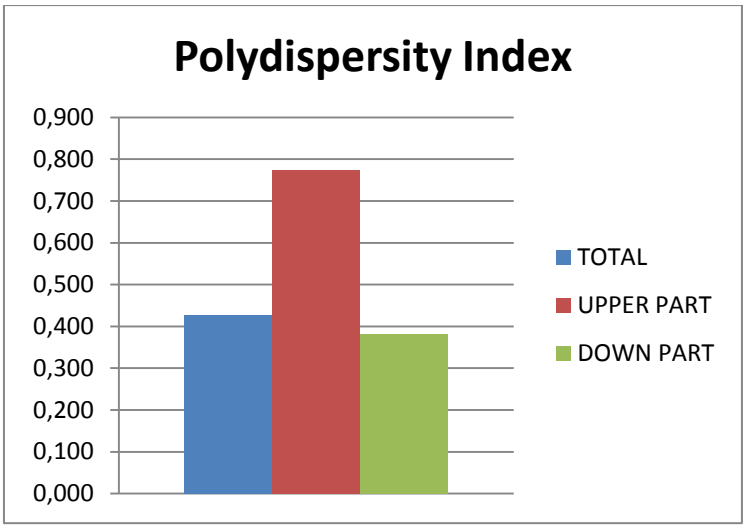

Figure 37 - Graphic representation of Size distribution of NanoParticles before (TOTAL) and after (UPPER and Down Part) filtration with a 3,000 MWCO.

From the measurements, we can corroborate that the 3,000 MWCO concentrator was useful to separate the obtained dispersion in two fractions: one containing agglomerates of CL and another one where Chitosan-dsDNA nanoparticles with size around 300nm obtained with a PI lower than 0.4.

Keep in mind:

- Chitosan-dsDNA nanoParticles could be formed using CL
- A 3,000 MWCO concentrator was useful to obtain Chitosan-dsDNA nanoparticles with size around 300nm and a PI lower than 0.4.

2.6 The role of surface charge

It is well establish that particles with high zeta potential of the same charge will repel each other. In general, a potential less than -30 mV and more than +30 mV is considered high. This is also the dividing line between stable and unstable suspensions. As said previously, for the range between these values there is no form to prevent molecules from coming together and flocculate (*60*).

There are some factors that have or might have an influence on zeta potential, like pH, the type of chitosan and the ionic strength of the medium.

In literature, the zeta potential of chitosan-DNA NanoParticles varies between 0 and 40mV at a pH of 5, 5 (*35, 60-61*). The majority of studies present a zeta potential of approximately 20mV and therefore they are considered unstable.

After using the filter with cut off of 3,000 MWCO, the potential zeta of the fraction containing the Chitosan-DNA Nanoparticles (upper part) has been studied. The measures were made in water, in order to avoid interferences with the ionic strength of the buffer (See table1). Two peaks, representative of the Chitosan-DNA nanoparticles (+ 18.8 mV) and the remaining DNA that is not entrap in the particles (- 2.26 mV) has been obtained.

Like chitosan, chitosan nanoparticles also possess a positive surface charge. This is explained by residual protonated amino groups of chitosan that do not take part in neutralisation with negatively charged DNA.

Table 1 - Zeta Potential

	Zeta Potential (mV)	SE
NP peak	18,8	1,42
DNA peak	-2,26	1,58

Keep in mind:

- Chitosan-dsDNA nanoparticles present a positive charge.
- Potential Zeta values of 18.8 put them on the border between stable and unstable suspensions.

2.7Interaction with blood and citotoxicity

When used as DNA carriers, understanding the interactions of the DNA-based particles with blood is crucial for improving their behaviour *in vitro* and *in vivo*. Although it had been suggested that chitosan is a biocompatible and nontoxic polymer, previous studies have revealed that soluble chitosan, like other cationic polymers, displayed concentration-dependent toxicity(*62*). The effect of these DNA-chitosan particles on both the membrane-lytic activity and their effect on cell viability were evaluated, respectively, by the hemolysis assay the tetrazolium salt MTT assay on 3T3 fibroblast cell lines.

2.7.1Haemolysis

Haemolysis is the rupturing of erythrocytes (red blood cells) and the release of their contents (hemoglobin) into surrounding fluid (*e.g.*, blood plasma). Haemolysis may occur *in vivo* or *in vitro* (inside or outside the body).

In order to test the interaction of CL and DNA/CL gel particles with blood, rat blood samples were used.

As is possible to verify in figure 38, the percentage of haemolysis in almost inexistent when the CL interacts with the blood

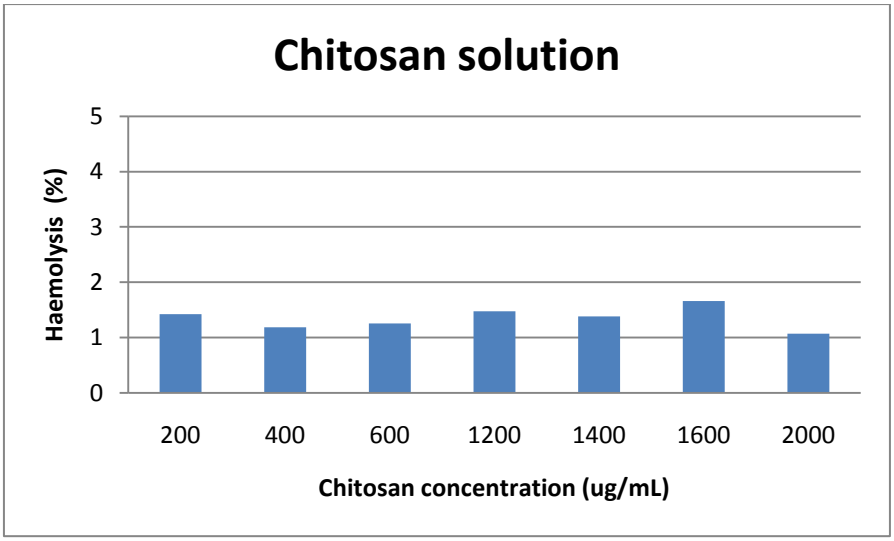

Figure 38 – Concentration dependence of Chitosan Lactate percentage of haemolysis.

A similar procedure was used to study CL-DNA gel particles. In this case, the influence of time on the haemolitic response has been evaluated. Although there is some fluctuation on the obtained values, as consequence of small differences, in sizes, between particles, it is important to note that in all cases the level of hemolysis is lower than 2%. (See figure 39)

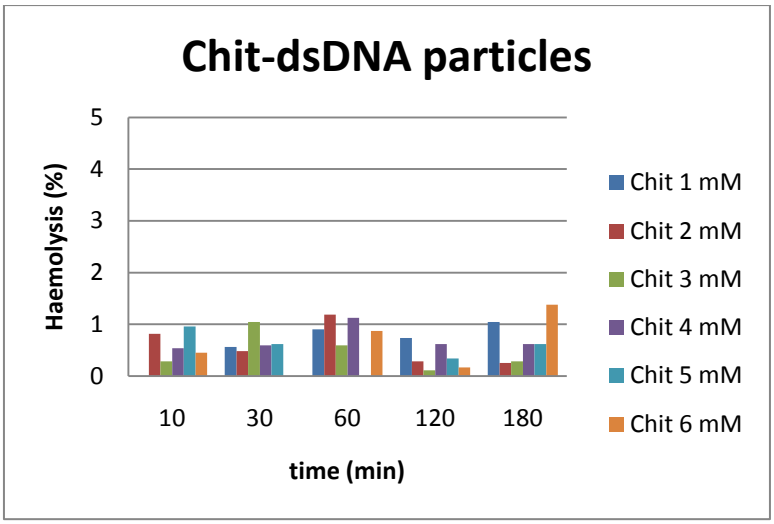

Figure 39 – Time dependence of CL-DNA particles in haemolysis response.

2.7.2 *In vitro* cytotoxicity

To evaluate the toxicity of our system on 3T3 fibroblast cell lines, it was tested first the chitosan lactate, than DNA/CL gel particles and for last NanoParticles. It is reported that CL showed the lowest cytotoxicity, compared with chitosan glutamate and chitosan hydrochloride, toward B16F10 cells(*63*). Studies with CL in COS-1 cells were also reported with good viability and CL as a safe gene carrier(*62*). On 3T3 fibroblast cell lines, for chitosan lactate solutions, the percentage of cell viability is always higher than 80% for a concentration up to 2, 00 μg/mL (Figure 40). Although it seems to be a tendency to decrease with the increment of chitosan lactate concentration, it is possible to confirm that the LC_{50} value for chitosan lactate is higher than 2, 00 μg/mL in the conditions studied in this work.

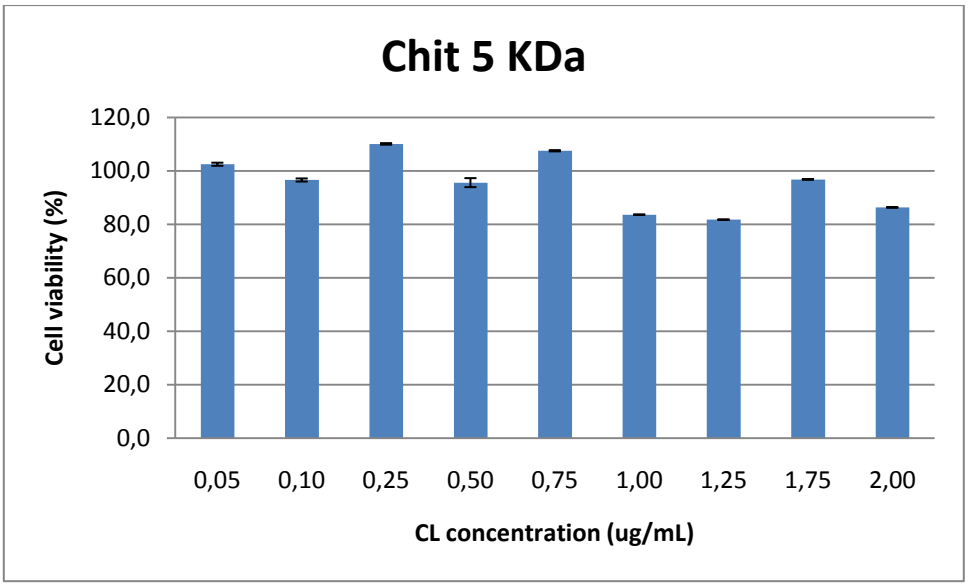

Figure 40 – Chitosan Lactate concentration behavior on cell viability.

It was expected that once CL present such a good viability, gel particles would also produce similar results. Figure 41 proves these assumptions. In fact, CL/DNA gel particles are quite viable, always higher than 80%.

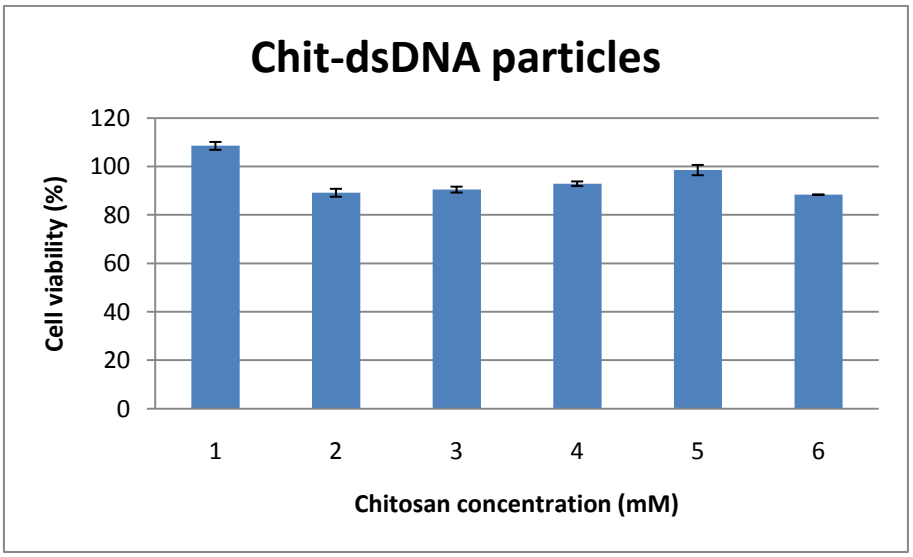

Figure 41 – CL-dsDNA particles concentration behavior on cell viability.

To study the toxicity of nanoparticles, see Figure 42, all the components of the concentrator were analyzed. The down part of the filter, in which more refined and monodisperse nanoparticles have been obtained, promote cell viabilities higher than 50 %, even for the highest concentration studies. With this data is possible to confirm that CL is a safe gene carrier on this cell line.

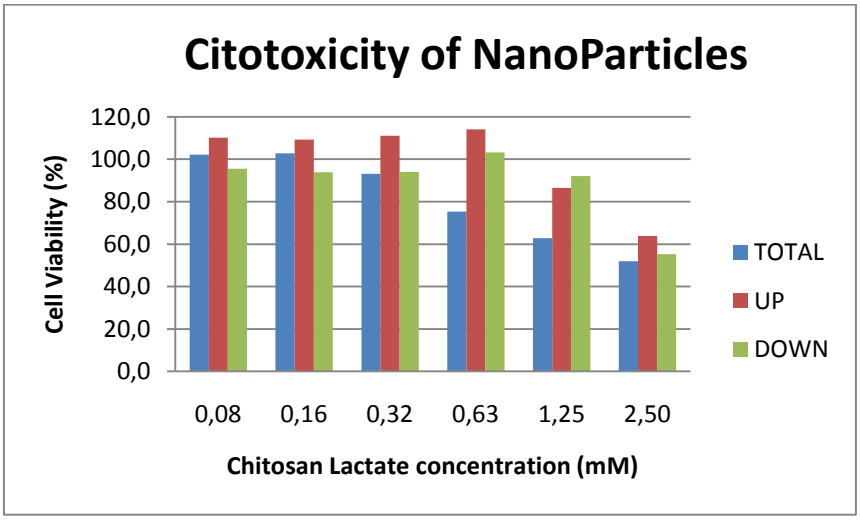

Figure 42 - CL-dsDNA nanoparticles concentration behavior on cell viability.

Analysis of the data indicates that chitosan lactate is a promising carrier to be used in the design and development of new non viral vectors for the delivery of therapeutic DNA.

Keep in mind:

- CL and CL-DNA Gel Particles provoke haemolysis lower than 2%, which can be regarded as non-toxic effect level.
- CL, CL-DNAGel Particles and CL-DNA Nanoparticles formed present excellent viability when used on 3T3 fibroblast cell lines.

Chapter 3.

Concluding remarks and Future Perspectives

On complexation studies:

- Particles size and opacity are indicative of the complexation´s degree, and are function of the concentration of CL.
- Besides the known drop size factor, the concentration of the cationic polyelectrolyte plays a crucial role in the size of the particles.

On Morphology and Structure studies:

- Secondary structure of DNA is kept in the particles.
- Chitosan Lactate can be visualized, when in excess, by Fluorescence Microscopy.
- It´s possible to find a tendency that show, that for concentration of Chitosan Lactate superior than 4mM, we have a transition from core-shell particles to solid particles.

On DNA complexation and Release studies:

- DNA is totally released from CL-dsDNA particles after 48 h.
- CL-dsDNA particles show LC values around 4%.

- Differences in viscosity of ssDNA and dsDNA solution could explain the instability of CL-ssDNA particles for the same range of CL concentrations.

On Nanoparticles studies:

- Chitosan-dsDNA nanoparticles can be formed using CL.
- The 3,000 MWCO concentrator was useful, to obtain Chitosan-dsDNA nanoparticles with size around 300nm and a PI lower than 0.4.

On The role of Surface Charge studies:

- Chitosan-dsDNA nanoparticles present a positive charge.
- Potential Zeta values of 18.8 put them on the border between stable and unstable suspensions.

On the Interaction with blood and Cytotoxicity studies:

- CL and CL-DNA Gel Particles provoke haemolysis lower than 2%, which can be regarded as non-toxic effect level.
- CL, CL-DNA Gel Particles and CL-DNA Nanoparticles formed present excellent viability when used on 3T3 fibroblast cell lines.
- CL is a promising efficient and safe gene carrier.

Thus, Chitosan Oligosaccharide Lactate (≈5kDa) is a promising safe and effective gene carrier.

The work is now focused on layer-by-layer particles using Alginate and Chitosan Lactate. With this strategy, it is expected to improve the content of DNA inside the particle, as well as form more stable particles.

Chapter 4.

Materials and experimental methods

4.1 Chapter Introduction

In this section it will be mentioned the materials used in this work and some important features of them, as well as the methods and techniques, that help us through the experimental part. It is also given a brief description of several techniques used, description which serves as support for the results obtained and discussed in this thesis.

4.2 Materials

4.2.1 Chitosan Lactate and its features

Chitosan Oligossacharide Lactate (CL) was purchased from Sigma Aldrich and used as received. CL has a mean molecular weight of approximately 5kDa. Other chitosans, with different molecular weights (150 kDa and 400 kDa), were also purchased from Sigma Aldrich and used to test the differences between them.

The fact that CL is soluble in water makes it extremely useful when worked with DNA. Chitosans of 150kDa and 400kDa and CL of ~ 5kDa were tested and left

to dissolve in water for 24 hours under stirring. In Figure 43, is presented the results for this simple solubility test for the Chitosan with 150kDa of molecular weight and CL.

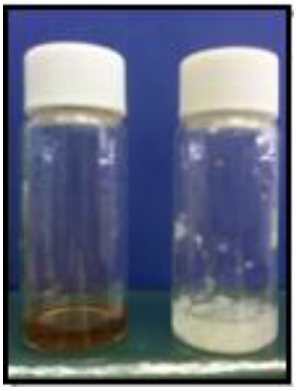

Figure 43 - Solubility of Chitosan Lactate and Chitosan´s solutions.

Only the solution of CL dissolved. The same behavior can be seen comparing CL with the 400 kDa molecular weight Chitosan. This happens because CL is already in a form of a salt, while Chitosan is a weak base, pKa value of the glucosamine residue is in the range between 6.2 and 7.0. Therefore it is insoluble in neutral and alkaline solutions and needs to be in an acidic medium, allowing the amino groups to be positively charged.

4.2.2 DNA

The sodium salt of deoxyribonucleic acid (DNA), from salmon testes of an average degree of polymerization of about 2000 base pairs, was purchased from Sigma and used as received. The ratios of absorbance at 260 and 280 nm of the stock solutions were found to be between 1.8 and 1.9, which suggested the absence of proteins.

4.3 Sample Preparation

4.3.1 Solutions preparation

Double Stranded DNA (dsDNA) stocks solutions were prepared in a 10mM NaBr solution in order to stabilize the DNA secondary structure in its native B-form conformation(*64*). Single Stranded DNA (ssDNA) solutions were prepared by heating of dsDNA solution for 15 minutes at a temperature of 85^0C and immediately immersed in an ice bath.

The CL solutions were prepared in a 1mL buffer of Tris HCl pH 7.6 (for potential zeta measures Chitosan Lactate was prepared in water).

4.3.2 Particles preparation

The formation of the CL-DNA particles was studied using mixtures of 60mM dsDNA and CL solutions ranging from 1 to 6mM. Gel Particles were formed through drop wise addition of the DNA solution into the CL solution. Particles were left in the mixing solution for 2 hours before any measure (See Figure 44).

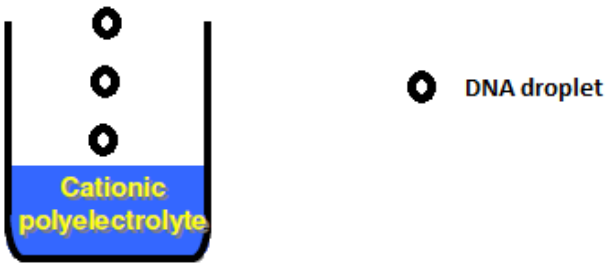

Figure 44 – Illustrative representation of DNA drop wise addition. In this case, the cationic polyelectrolyte is Chitosan Lactate.

4.3.3 Nanoparticles preparation

Particles were prepared at a charge ratio between DNA and cationic agent equal to 1, R = [DNA]/ [CL], where [CL] is the concentration of Chitosan Lactate. [DNA] was equal to 5 mM, once higher concentrations of DNA produce high viscosity solutions, which make them inconvenient systems for the nebulisation process. The used comp Air-we-28-E nebuliser, illustrated in Figure 45, enables the generation of very fine droplets/aerosols (*59*). The solutions were nebulised into gently stirred Chitosan Lactate solutions.

Figure 45 - Comp Air-we-28-E nebulizer.

4.4 Methods and Procedures

4.4.1 For Morphology and structure studies

4.4.1.1 Fluorescence microscopy

Fluorescence is the result of a three-stage process that occurs in certain molecules (generally polyaromatic hydrocarbons or heterocycles) called fluorophores or fluorescent dyes. A fluorescent probe is a fluorophore designed

to respond to a specific stimulus or to localize within a specific region of a biological specimen(*65*). The process responsible for the fluorescence of fluorescent probes and other fluorophores is illustrated by the simple electronic-state diagram (Jablonski diagram) shown in Figure 46.

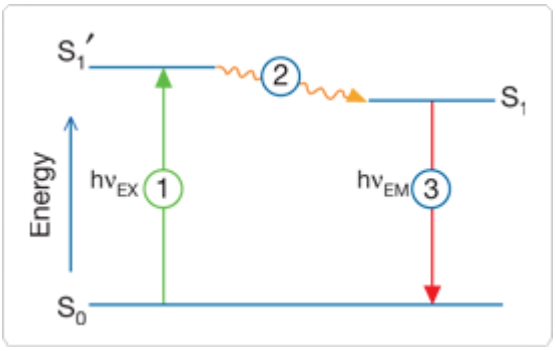

Figure 46 – Electronic-state diagram.

Stage 1: Excitation

A photon of energy $h\nu_{EX}$ is supplied by an external source such as an incandescent lamp or a laser and absorbed by the fluorophore, creating an excited electronic singlet state (S_1'). This process distinguishes fluorescence from chemiluminescence, in which the excited state is populated by a chemical reaction.

Stage 2: Excited-State Lifetime

The excited state exists for a finite time (typically 1–10 nanoseconds). During this time, the fluorophore undergoes conformational changes and is also subject to a multitude of possible interactions with its molecular environment. These processes have two important consequences. First, the energy of S_1 is partially dissipated, yielding a relaxed singlet excited state (S_1) from which fluorescence emission originates. Second, not all the molecules initially excited by absorption (Stage 1) return to the ground state (S_0) by fluorescence emission. Other processes such as collisional quenching, fluorescence resonance energy transfer

(FRET) (Fluorescence Resonance Energy Transfer) and intersystem crossing may also depopulate S_1.

Stage 3: Fluorescence Emission

A photon of energy $h\nu_{EM}$ is emitted, returning the fluorophore to its ground state S_0. Due to energy dissipation during the excited-state lifetime, the energy of this photon is lower, and therefore of longer wavelength, than the excitation photon $h\nu_{EX}$. The difference in energy or wavelength represented by ($h\nu_{EX}$ – $h\nu_{EM}$) is called the Stokes shift. The Stokes shift is fundamental to the sensitivity of fluorescence techniques because it allows emission photons to be detected against a low background, isolated from excitation photons.

Procedure

Information about the secondary structure of the DNA molecules in the gels was obtained by fluorescence microscopy, using N, N, N´, N´-tetramethylacridine-3, 6-diamine (acridine orange, AO), represented in Figure 47, as the staining medium. Acridine orange has been used to label nucleic acids in solution and intact cells. Acridine orange intercalates into double-stranded DNA as a monomer, whereas it binds to single-stranded DNA as an aggregate.

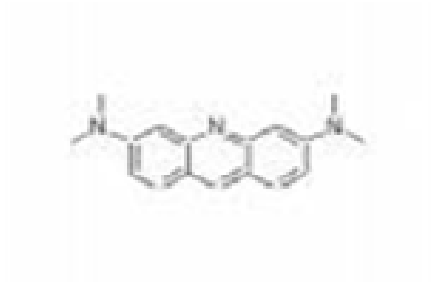

Figure 47 – Chemical Structure of Acridine Orange.

Upon excitation at 470-490 nm, the monomeric acridine orange bound to double-stranded DNA fluoresces green, with an emission maximum at 530 nm.

The aggregated acridine orange on single stranded DNA fluoresces red, with an emission at about 640 nm (*66*).

For analyzing the nanoparticles, DNA solutions were nebulised and collected into gently stirred CL solution. After that, dispersions were stained with Acridine Orange to confirm the presence of DNA in the particles. In addition, using AO, information about the secondary structure of the nucleic acid in the particles has been obtained.

The stained suspensions were immediately examined with an Olympus BX51Mmicroscope equipped with a UV-mercury lamp (100WUshio Olympus) and a filter set type U-MNIBA (470 – 495 nm excitation and 505 nm dichromatic mirror). The DNA gel particles were observed using an UplanFL N 100x/1.30 oil-immersed objective lens (∞/0.17/FN26.5). Images were digitized on a computer through a video camera (Olympus digital camera DP70) and were analyzed with an image processor (OlympusDP Controller 2.1.1.176, Olympus DP Manager 2.1.1.158).

4.4.1.2 Scanning electron microscopy (SEM)

Accelerated electrons in a SEM carry significant amounts of kinetic energy, and this energy is dissipated as a variety of signals produced by electron-sample interactions when the incident electrons are decelerated in the solid sample. These signals include secondary electrons (that produce SEM images), backscattered electrons (BSE), diffracted backscattered electrons (EBSD) that are used to determine crystal structures and orientations of minerals), photons, visible light and heat. Secondary electrons and backscattered electrons are commonly used for imaging samples: secondary electrons are most valuable for showing morphology and topography on samples and backscattered electrons are most valuable for illustrating contrasts in composition in multiphase samples (i.e. for rapid phase discrimination)(*67*). X-ray generation is produced by inelastic

collisions of the incident electrons with electrons in discrete orbital of atoms in the sample. As the excited electrons return to lower energy states, they yield X-rays that are of a fixed wavelength (that is related to the difference in energy levels of electrons in different shells for a given element). Thus, characteristic X-rays are produced for each element in a mineral that is "excited" by the electron beam. A schematic illustration of SEM is shown in Figure 48.

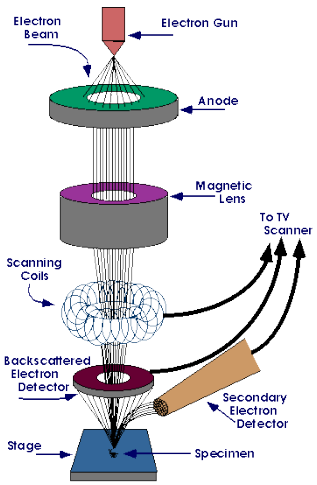

Figure 48 – Schematic illustration of SEM.

Procedure

Sample preparation is usually not very invasive and results can be obtained quickly. For SEM, a sample preparation is necessary and only solid samples can be viewed with this technique. Thus, solutions containing the particles were freeze-dried overnight (-46 ^{0}C, 0.035 mBar). The dry samples were sprinkled on a double sided adhesive conductive carbon tape attached to a SEM stub. After sputter coating with gold, the samples were transferred onto the microscope stage and examined at 5 kV. The lyophilization procedure constitutes a standard protocol for the preparation of samples prior to their examination by means of SEM.

4.4.2 For DNA release studies

4.4.2.1 UV-VIS spectroscopy

The visible region of the spectrum comprises photon energies of 36 to 72 kcal/mole, and the near ultraviolet region, out to 200 nm, extends this energy range to 143 kcal/mole. Ultraviolet radiation having wavelengths less than 200 nm is difficult to handle, and is seldom used as a routine tool for structural analysis (*68*).

The energies noted above are sufficient to promote or excite a molecular electron to a higher energy orbital. Consequently, absorption spectroscopy carried out in this region is sometimes called "electronic spectroscopy". A diagram showing the various kinds of electronic excitation that may occur in organic molecules is shown in Figure 49.

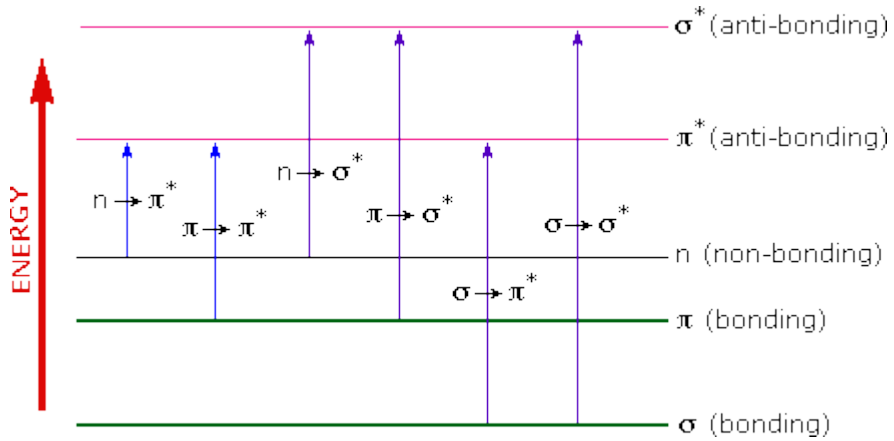

Figure 49 - Various kinds of electronic excitation that may occur in organic molecules.

Of the six transitions outlined, only the two lowest energy ones (left-most, colored blue) are achieved by the energies available in the 200 to 800 nm spectrum. As a rule, energetically favored electron promotion will be from the highest occupied molecular orbital (HOMO) to the lowest unoccupied molecular orbital (LUMO), and the resulting species is called an excited state.

When sample molecules are exposed to light having an energy that matches a possible electronic transition within the molecule, some of the light energy will be absorbed as the electron is promoted to a higher energy orbital. An optical spectrometer records the wavelengths at which absorption occurs, together with the degree of absorption at each wavelength. The resulting spectrum is presented in a plot of absorbance (A) versus wavelength.

Because the absorbance of a sample will be proportional to the number of absorbing molecules in the spectrometer light beam (e.g. their molar concentration in the sample tube), it is necessary to correct the absorbance value for this and other operational factors if the spectra of different compounds are to be compared in a meaningful way. The corrected absorption value is called "molar absorptivity", and is particularly useful when comparing the spectra of different compounds and determining the relative strength of light absorbing functions (chromophores). Molar absorptivity (ε) is defined in Equation 1:

$$\varepsilon = A \div (l.c) \quad \textbf{Equation 1}$$

Where *A* is the absorbance, c is the sample concentration in moles/liter and l is the length of light path through the sample in cm.

Procedure

DNA release studies, from the gel particles, were carried out. Hence, at defined time intervals, the supernatant was collected and particles were resuspended in a fresh solution. The DNA released into the supernatant solutions was quantified by measuring the absorbance at 260 nm with a spectrophotometer (UV/VIS spectrophotometer V-530 JASCO).

4.4.3 For Nanoparticles size studies

4.4.3.1 Dynamic light scattering

Dynamic light scattering (DLS), which is also called quasielastic light scattering (QELS) or photon correlation spectroscopy (PCS), is a widely used method for the determination of the dynamics of colloidal systems and diffusion coefficients therein. It was developed in the 1960s. In the fifty years since its inception, modern dynamic light scattering techniques have become increasingly sophisticated, and their applications have grown exceedingly diverse. Applications of the techniques to problems in physics, chemistry, biology, medicine, and fluid mechanics have proliferated (*69*).

Briefly, when light impinges on matter, the electric field of the light induces an oscillating polarization of the electrons in the molecules of the particles.

The particles then serve as secondary sources of light and subsequently radiate (scatter) light. When the source of light is coherent and monochromatic, as from a laser with a wavelength, λ, and incident intensity, $I0$, it is possible to observe time-dependent fluctuations in the scattered intensity, I, at a certain distance, r, and angle θ, using a suitable detector, such as a photomultiplier, capable of operating in photon counting mode.

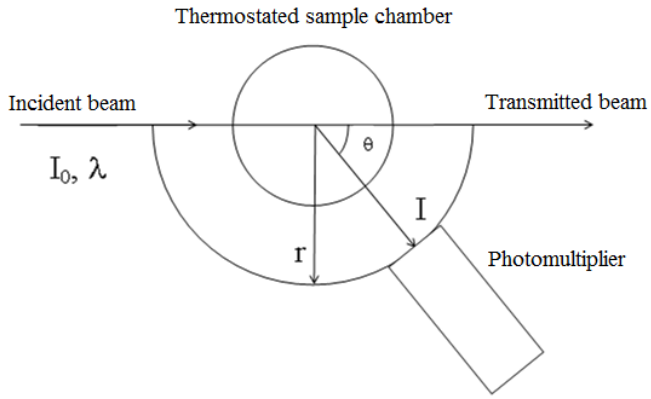

Figure 50 – Layout of a light scattering spectrometer.

The time-dependent fluctuations arise from the fact that the particles are small enough as to undergo random thermal (Brownian) motion and the distance between them is therefore constantly varying. Constructive and destructive interference of light scattered by neighboring particles within the illuminated zone gives rise to the intensity fluctuation at the detector plane which, as it arises from particle motion, contains information of this motion.

When the particles are very small compared to the wavelength of the light, the intensity of the scattered light is uniform in all directions (Rayleigh scattering); whereas for larger particles (diameter ≥ 250 nm), the intensity is angle-dependent (Mie scattering).

The frequency shifts, the angular distribution, the polarization, and the intensity of the scattered light are determined by the size, shape, and molecular interactions in the scattering material. Thus from the light scattering characteristics of a given system it is possible, with the aid of electrodynamics and theory of time-dependent statistical mechanics, to obtain information about the structure and molecular dynamics of the scattering medium.

Procedure

To examine the size distribution, of the DNA gel particles, PCS experiments were carried out. PCS is a very fast, absolute and non-destructive particle sizing technique. PCS measurements performed at 20^0C with a detection angle of 90^o yielded the size distributions.

4.4.4 For Particles charge studies

4.4.4.1 Zeta Potential

Although it is mentioned that particles are electrically charged it is important to realize that the charge on the surface of each particle is counterbalanced by charges (ions) of opposite sign in the surrounding solution. The suspension is neutral overall and also on a scale somewhat larger than the particles themselves.

The charges on the particle surface are normally considered to be attached rather firmly to it and to remain there more or less indefinitely (though they may be exchanging with charges of similar type in the solution). The surrounding (balancing) charges, in contrast, are much more loosely associated with the particle.

Ions close to the surface of the particle, will be strongly bound while ions that are further away will be loosely bound forming what is called the diffuse layer.

Within the diffuse layer there is a motional boundary and any ions within this boundary will move with the particle when it moves in the liquid; but any ions outside the boundary will stay where they are – this boundary is called the slipping plane (See Figure 51).

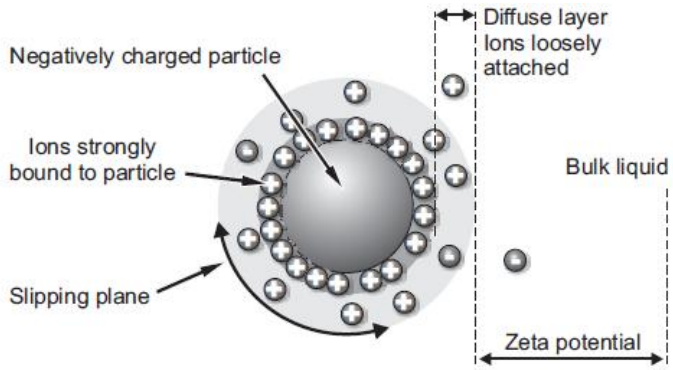

Figure 51 – Schematic representation of the electrical double-layer (adapted from zetasizer manual).

The electrostatic potential on that surface is called the zeta potential (*70*)and it is that potential which is measured, when one measures the velocity of the particles in a direct current electric field.

When the charge is measured in this way it reflects more realistically what one particle "sees" as it approaches another particle and that is what determines the properties of the suspension. If the repulsion between approaching particles is large enough they will bounce away from one another and that will keep the particles in a state of dispersion. If the repulsive force is not strong enough, the particles will come together and may stick in a permanent doublet. Then other particles may come along and also be caught in the growing aggregate.

The suspension is then unstable and the aggregates will quickly settle out from the surrounding medium. If one is relying on the electric charge alone to keep the system in a disperse state then the zeta potential will usually need to be kept above 25 mV (positive or negative) (*71*).

Generally speaking, the higher the absolute value of the zeta potential, the more stable the system will be. That means that the system will be better able to withstand additions of salt (which might otherwise destabilize it). It will also usually show a lower viscosity.

4.4.4.2 Electrophoresis in agarose gel

The term electrophoresis is generally applied to the movement of small ions and charged macromolecules in solution under the influence of an electric field. The rate of migration depends on the size, charge and shape of the molecule, the applied current and the resistance of the medium.(*72*) When placed in semi-permeable media, like an agarose gel, DNA will follow the electric field and will reptate throughout the gel. Larger fragments migrate more slowly, in a rate approximately proportional to its charge to mass ratio, towards the positive electrode. The position of DNA in the gel is detected using fluorescent dyes, such as Gelstar®. The electrophoresis must be performed in a buffer solution. The most commonly buffer used in the gel electrophoresis of DNA is TBE (Tris-Borate-EDTA, pH 8.2). This buffer not only establishes the pH even at relatively high temperatures, but provides sufficient ions to support conductivity.

Procedure

Agarose (0.7g) was dissolved in TBE buffer (100mL) by heating until boiling and was afterwards allowed to cool down. 5µL of a 10,000× solution of Gelstar® was added to the agarose solution which was then poured into a 10 by 20cm gel tank. Air bubbles were removed with a pipette tip and the gel comb was added to the gel which was allowed to set. The DNA-CL particles prepared following the previously mentioned protocol were added to each sample wells. The electrophoresis was carried out in a horizontal tank containing TBE buffer and was run at 90 V for 1 hour. Gels were imaged using a UV transilluminator.

4.4.5 For DNA viscosity studies

Rheology is the branch of fluid mechanics that studies the physical properties that influence the amount of transport of fluid motion, that is, refers to the study of flow and deformation behavior of matter, or fluidity.

In this type of test, it is assumed that the material flow, by application of stress, then the response is measured over time or temperature.

The rotational speed depends on the viscosity of the sample, which is calculated using the stress and the shear rate.

Viscosity is traditionally regarded as the most important material property and any practical study requiring knowledge of material´s response would automatically turn to the viscosity in the first instance. The concept was introduced through Newton´s postulate. The lack of slipperiness described by Newton is what it is called "viscosity". It is synonymous with internal friction and is measure of resistance to flow. The force per unit area required to produce the motion, F/A, is denoted by the shear stress, σ, and is proportional to the velocity gradient, or shear rate, ў. The constant of proportionality, η, is called viscosity (Equation 2):

$$\sigma = \eta \,.\breve{y} \quad \textbf{Equation 2}$$

4.4.6 For studies of cytotoxicity and haemolysis

4.4.6.1 Haemolysis

Determination of haemolytic properties is one of the most common tests in studies of nanoparticle interaction with blood components. Interpreting the

results of these studies is complicated due to variability in experimental approaches and a lack of universally accepted criteria for determination of the test-result validity. Most *in vitro* studies of particle-induced hemolysis evaluate the percentage hemolysis by spectrophotometriclly detecting plasma free hemoglobin derivatives after incubating the particles with blood and then separating undamaged cells by centrifugation (*73*). The incubation time, wavelength at which hemoglobin is quantified and blood conditions (e.g. use of purified erythrocytes rather than whole blood, and inclusion of various anti-coagulants) vary significantly from one study to another. In addition to these variables, differences in relative centrifugal force, blood storage time and conditions, blood sources (human, rabbit or mouse) can further complicate meaningful comparison of the results from disparate studies.

Procedure

Preparation of red blood cells suspensions:

Rat blood was obtained from the anaesthetized animals, by cardiac puncture, and drawn into tubes containing EDTA. The procedure is approved by the institutional ethics committee on animal experimentation. The serum was removed from the blood by centrifugation at 3,000 rpm (Megafuge 2.0 R Heraeus Instruments) at 4^0 C for 10 min, and subsequent suction. The red blood cells were then washed three times at 4 ° C by centrifugation at 3,000 rpm with isotonic saline PBS solution, containing 22.2 mmol/L Na_2HPO_4, 5.6 mmol/L KH_2PO_4, 123.3 mmol/L NaCl in distilled water (pH 7.4). Following the last wash, the cells were diluted to ½ of their volume with isotonic PBS solution (cell density of 8 x 10^9 cell/mL)

Hemolysis assay**:**

The membrane-lytic activity of the systems was examined by hemolysis assay. Firstly, the haemolytic response of chitosan lactate (CL) in solution was tested.

Thus, a series of different volumes of CL solution (10 mg/mL), ranging from 10 to 200 μL, were placed in polystyrene tubes and an aliquot of 25 μL of erythrocyte suspension was added to each tube. The final volume is 1 mL. The tubes were incubated at room temperature for 10 min under shaking conditions. Following incubation, the tubes were centrifugated (5 min at 10, 000 rpm). The haemolysis degree was determined by comparing the absorbance (540 nm) (Shimadzu UV-160A) of the supernatant with that of the control samples totally haemolysed with distilled water. Positive and negative controls were obtained by adding an aliquot of 25 μl of erythrocyte syspension to bidistilled water and isotonic PBS solution, respectively.

In the case of DNA particles, individual DNA gel particles were placed in the tubes and an aliquot of 25 μL or erythrocyte suspension was added to each tube. The final volume is 1 mL. The tubes were incubated at room temperature for different times under shaking conditions. At defined times; the incubated samples were centrifuged (5 min at 10, 000 rpm). The haemolysis degree was determined following the same procedure as described above.

4.4.6.2 *In vitro* cytotoxicity

The *in vitro* toxicity testing is the scientific analysis of the effects of toxic chemical substances on cultured bacteria or mammalian cells. *In vitro* (literally 'in glass') testing methods are employed primarily to identify potentially hazardous chemicals and/or to confirm the lack of certain toxic properties in the early stages of the development of potentially useful new substances such as therapeutic drugs, agricultural chemicals and direct food additives that may or may not taste good. The *in vitro* cell viability (cytotoxicity) assays are used to refrain the unneeded use of animal testing. *In vitro* assays are also faster and cheaper to conduct, therefore suitable for testing of large number of different compounds and samples.

The mechanisms of cell death include apoptosis and necrosis. The amount of cell death induced by different agents can be measured on various methods (*74*).

MTT assay

MTT assay (representative image of the MTT assay used on the present work, is shown in Figure 52) is a sensitive quantitative colorimetric assay measuring the reduction of yellow tetrazolium salt MTT to dark purple formazan by succinate dehydrogenase enzime, mainly in mitochondria. Reduction of MTT to formazan happens only in metabolically active cells and thus can be used to measure the viability of the cells.

Lactate dehydrogenase assay

Lactate dehydrogenase (LDH) cytotoxicity assay measures the activity of a cytosolic LDH enzyme. The studied substance is applied on the cells and increased LDH activity correlates with increased cell wall damage and LDH leakage to extracellular space, thus acting as an indicator of cell membrane integrity. Like in MTT assay, tetrazolium salt is involved in the colorimetric reaction where LDH activity leads to formation of formazan which is then detected spectrophotometrically.

Neutral read assay

The neutral red (NR) assay is based on the ability of viable cells to incorporate and bind neutral red within lysosomes. Neutral red penetrates cell membrane and accumulates in lysosomal matrix. Changes on the cell surface of the sensitive lysosomal membrane lead to lysosomal fragility and inability to uptake and store neutral red. Neutral red assay is measured quantitatively with a spectrophotometer.

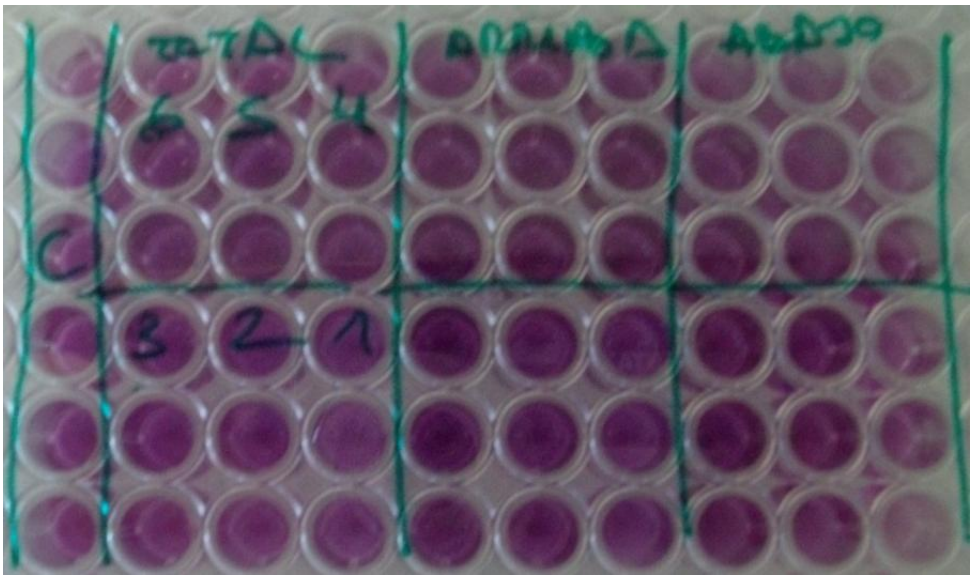

Figure 52 – *In vitro* toxicity studies made in this work, using the MTT assay.

Procedure

Cell culture:

The murine Swiss albino 3T3 fibroblast cell line was grown in DMEM medium (4,5 $g.l^{-1}$ glucose) supplemented with 10% (v/v) FBS, 2 mM L-glutamine, 100 U ml-1 penicillin and 100 μg ml-1 streptomycin at 37 ^{0}C, 5% CO2. The 3T3 cells were routinely cultured in 75 cm2 culture flasks and were trypsinized using trypsin-EDTA when the cells reached approximately 80% confluence.

Cytotoxicity assays:

The cytotoxic effect of the systems was measured by tetrazolium salt MTT assay. 3T3 cells were seeded into the central 60 wells of a 96-well plate at a density of 5 x 104 cells ml^{-1}. After incubation for 24 h under 5% CO_2 at 37 ^{0}C, the spent medium was replaced with 100 μl of fresh medium supplemented with 5% FBS

containing chitosan lactate solution at the required concentration range (50-2000 μg ml-1).

In the case of DNA particles, individual DNA gel particles were placed in the wells. After 24 h, the medium was removed, and 100 μl of MTT in PBS (5 mg ml-1) diluted 1:10 in medium without FBS and phenol red was then added to the cells.

The plates were further incubated for 3 h, after which the medium was removed, and the cells were washed once in PBS. Thereafter, 100 μl of DMSO was then added to each well to dissolve the purple formazan product (MTT assay). After 10 min on a microtitre-plate shaker at room temperature, the absorbance of the resulting solutions was measured at 550 nm using a Bio-Rad 550 microplate reader. The effect of each treatment was calculated as a percentage of cell viability inhibition against the respective controls.

References

1. F. Oosawa, *Polyelectrolytes*. (Marcel Dekker Inc., New York, 1971).

2. Y. S. Mel'nikova, Lund University (2000).

3. E. S. Doi M, *The theory of polymer dynamics*. (Clarendon Press, Oxford, 1989).

4. C. R. Rubinstein M, *Polymer physics*. (Oxford University Press, New York, 2003).

5. R. R. Sinden, *DNA Structure and Function*. (Academy Press Inc., California, 1994).

6. J. S. a. J. W. J. Inglis, *Inspiring science: Jim Watson and the age of DNA*. (Cold Spring Harbor, New York, 2003).

7. M. O. K. a. B. Jönsson, **49**, 121 (1999).

8. L. W. C. Leal, G. Olofsson, M. Miguel and H. Wennerström *J. Phys. Chem. B* **108**, 3044 (2004).

9. M. G. a. J. P. Demaret, *Proc. Natl. Acad. Sci.* **89**, 5740 (1992).

10. M. Rosa, Universidade de Coimbra (2006).

11. D. Voet, Voet, J.G., *Biochemistry*. (John Wiley & Sons, Inc., New York, ed. Second Edition, 1994).

12. M. Campbell, Farrel,S., *Biochemistry*. (Thomson Brooks/Cole, ed. Sixth, 2009).

13. X. Zhang, W. T. Godbey, *Advanced Drug Delivery Reviews* **58**, 515 (2006).

14. A. El-Aneed, *J. Control. Release* **94**, 1 (2004).

15. S. Mansouri *et al.*, *European Journal of Pharmaceutics and Biopharmaceutics* **57**, 1 (2004).

16. S. Mao, W. Sun, T. Kissel, *Advanced Drug Delivery Reviews* **62**, 12 (2010).

17. J. K. a. T. K. T. Merdan, *Adv. Drug Deliv. Rev.* **54**, 715 (2002).
18. B. L. R. S. Dias, *DNA Interactions with Polymers and Surfactants*. (Wiley, Hoboken,, 2008).

19. L. Xianghui, Winsconsin-Madison (2008).

20. M. N. V. Ravi Kumar, *Reactive and Functional Polymers.Elsevier* **46**, 1 ((2000)).

21. K. Romøren, A. Aaberge, G. Smistad, B. J. Thu, Ø. Evensen, *Pharmaceutical Research* **21**, 2340 (2004).

22. C. K. S. Pillai, W. Paul, C. P. Sharma, *Progress in Polymer Science* **34**, 641 (2009).

23. G. E. W. G. L. Bowlin, M. Dekker, Ed. (New York 2004).

24. Y. Shin, *J.Appl.Polym.Sci.* **74**, 2991 (1999).

25. S. Hirano, *Biochem. Syst.Ecol.* **19**, 379 (1991).

26. A. D. Sezer, Akbuga, J., *J. Microencapsulation* **16**, 687 (1999).

27. M. M. Aranaz I, Harris R, Paños I, Miralles B, Acosta N, Galed G, Heras Á, *Current Chemical Biology* **3**, 203 (2009).

28. D. Alain, D. Monique, in *Polymeric Biomaterials, Revised and Expanded.* (CRC Press, 2001).

29. W. J. Mumper R.J., Claspell J.M., Rolland A.P., paper presented at the Proceedings of the Controlled Release Society, 1995.

30. M. Köping-Höggård, Y. S. Mel'nikova, K. M. Vårum, B. Lindman, P. Artursson, *The Journal of Gene Medicine* **5**, 130 (2003).

31. T. Sato, T. Ishii, Y. Okahata, *Biomaterials* **22**, 2075 (2001).

32. K. Romøren, S. Pedersen, G. Smistad, Ø. Evensen, B. J. Thu, *International Journal of Pharmaceutics* **261**, 115 (2003).

33. W. Liu *et al.*, *Biomaterials* **26**, 2705 (2005).

34. M. Lavertu, S. Méthot, N. Tran-Khanh, M. D. Buschmann, *Biomaterials* **27**, 4815 (2006).

35. M. Huang, C.-W. Fong, E. Khor, L.-Y. Lim, *Journal of Controlled Release* **106**, 391 (2005).

36. M. Koping-Hoggard *et al.*, *Gene Ther* **11**, 1441 (2004).

37. S.-i. Aiba, *International Journal of Biological Macromolecules* **11**, 249 (1989).

38. B. J. Krister Holmberg, Bengt Kronberg, Bjorn Lindman, *Surfactants and Polymers in Aqueous Solution*. (John Wiley & Sons, Ltd, 2002).

39. L. Piculell, B. Lindman, *Advances in Colloid and Interface Science* **41**, 149 (1992).

40. M. Laudon *et al.* (Clean Technology and Sustainable Industries Organization ; CRC Press ; CSI Events, Boston; Boca Raton, Fla.; Danville, Calif.).

41. R. C. Merkle, *Nanotechnology and Medicine, Advances in Anti-Aging Medicine*. (Dr. Ronald M. Klatz, Liebert press, 1996), vol. I.

42. R. A. Freitas, *Studies In Health Technology And Informatics* **80**, 45 (2002).
43. W. Tiyaboonchai, *Naresuan University Journal* **11**, 51 (2003).

44. S. Danielsen, K. M. Vårum, B. T. Stokke, *Biomacromolecules* **5**, 928 (2004).

45. G. Maurstad, S. Danielsen, B. T. Stokke, *Biomacromolecules* **8**, 1124 (2007).

46. S. P. Strand *et al.*, *Biomaterials* **31**, 975 (2010).

47. M. Hashimoto, M. Morimoto, H. Saimoto, Y. Shigemasa, T. Sato, *Bioconjugate Chemistry* **17**, 309 (2006).

48. M. M. Issa *et al.*, *Journal of Controlled Release* **115**, 103 (2006).

49. S. Mao *et al.*, *Biomaterials* **26**, 6343 (2005).

50. Y. Zhang *et al.*, *Biotechnology and Applied Biochemistry* **46**, 197 (2007).

51. T. Kean, S. Roth, M. Thanou, *Journal of Controlled Release* **103**, 643 (2005).
52. M. C. Morán, M. G. Miguel, B. Lindman, *Biomacromolecules* **8**, 3886 (2007).

53. Y. Lapitsky, W. J. Eskuchen, E. W. Kaler, *Langmuir* **22**, 6375 (2006).

54. Y. Lapitsky, E. W. Kaler, *Colloids and Surfaces A: Physicochemical and Engineering Aspects* **250**, 179 (2004).

55. J. Rejman, V. Oberle, I. S. Zuhorn, D. Hoekstra, *Biochem. J.* **377**, 159 (Jan 1, 2004, 2004).
56. O. N. M. McCallion, K. M. G. Taylor, P. A. Bridges, M. Thomas, A. J. Taylor, *International Journal of Pharmaceutics* **130**, 1 (1996).
57. C. Rudolph *et al.*, *Pharmaceutical Research* **21**, 1662 (2004).
58. A. T. Florence, A. M. Hillery, N. Hussain, P. U. Jani, *Journal of Controlled Release* **36**, 39 (1995).
59. M. C. Moran, F. R. Baptista, A. Ramalho, M. G. Miguel, B. Lindman, *Soft Matter* **5**, 2538 (2009).
60. H.-Q. Mao *et al.*, *Journal of Controlled Release* **70**, 399 (2001).
61. D.-W. Lee, K. Powers, R. Baney, *Carbohydrate Polymers* **58**, 371 (2004).
62. W. Weecharangsan, P. Opanasopit, T. Ngawhirunpat, T. Rojanarata, A. Apirakaramwong, *AAPS PharmSciTech* **7**, E74 (2006).
63. B. Carreño-Gómez, R. Duncan, *International Journal of Pharmaceutics* **148**, 231 (1997).
64. M. C. Morán, Graça Miguel, M. , Lindman. B., *Langmuir* **23**, 6478 (2007).
65. J. R. Lakowicz, *Principles of Fluorescence Spectroscopy*. (Springer, New York, ed. Third, 2006).
66. A. Peacocke, *Interscience Publishers*, 723 (1973).
67. R. F. Egerton, *Springer*, 202 (2005).
68. D. Skoog, Holler, F. , Nieman, T. , *Princípios de Análise Instrumental*. (Bookman, São Paulo, ed. Fifth, 2002).
69. B. J. Berne, Pecora, R. , *Dynamic Light Scattering*. (John Wiley & Sons, New York, 1976).
70. R. J. Hunter, *Academic Press*, (1981).
71. A. V. Delgado, F. González-Caballero, R. J. Hunter, L. K. Koopal, J. Lyklema, *Journal of Colloid and Interface Science* **309**, 194 (2007).
72. W. Fitschen, *Biochemical Education* **19**, 102 (1991).
73. B. W. Neun, M. A. Dobrovolskaia. (2009), vol. 697, pp. 215-224.
74. T. Mosmann, *Journal of Immunological Methods* **65**, 55 (1983).